
FEDERATED LEARNING WITH DYNAMIC CLIENT ARRIVAL AND DEPARTURE: CONVERGENCE AND RAPID ADAPTATION VIA INITIAL MODEL CONSTRUCTION

Zhan-Lun Chang

Elmore Family School of Electrical and Computer Engineering
Purdue University
West Lafayette, IN 47907, US
chang837@purdue.edu

Dong-Jun Han

Department of Computer Science and Engineering
Yonsei University
Seoul, South Korea
djh@yonsei.ac.kr

Rohit Parasnis

The Laboratory for Information and Decision Systems
Massachusetts Institute of Technology
Cambridge, MA 02139, US
rohit100@mit.edu

Seyyedali Hosseinalipour

Department of Electrical Engineering
University at Buffalo-SUNY
Buffalo, NY 14260, US
alipour@buffalo.edu

Christopher G. Brinton

Elmore Family School of Electrical and Computer Engineering
Purdue University
West Lafayette, IN 47907, US
cgb@purdue.edu

ABSTRACT

While most existing federated learning (FL) approaches assume a fixed set of clients in the system, in practice, clients can dynamically leave or join the system depending on their needs or interest in the specific task. This dynamic FL setting introduces several key challenges: (1) the objective function dynamically changes depending on the current set of clients, unlike traditional FL approaches that maintain a static optimization goal; (2) the current global model may not serve as the best initial point for the next FL rounds and could potentially lead to slow adaptation, given the possibility of clients leaving or joining the system. In this paper, we consider a dynamic optimization objective in FL that seeks the optimal model tailored to the currently active set of clients. Building on our probabilistic framework that provides direct insights into how the arrival and departure of different types of clients influence the shifts in optimal points, we establish an upper bound on the optimality gap, accounting for factors such as stochastic gradient noise, local training iterations, non-IIDness of data distribution, and deviations between optimal points caused by dynamic client pattern. We also propose an adaptive initial model construction strategy that employs weighted averaging

guided by gradient similarity, prioritizing models trained on clients whose data characteristics align closely with the current one, thereby enhancing adaptability to the current clients. The proposed approach is validated on various datasets and FL algorithms, demonstrating robust performance across diverse client arrival and departure patterns, underscoring its effectiveness in dynamic FL environments.

1 INTRODUCTION

Federated learning (FL) is a decentralized machine learning paradigm that facilitates collaborative model training across multiple clients, such as smartphones and Internet of Things (IoT) clients, without exchanging individual data. Instead of transmitting raw data to the central server, each client performs local training using its proprietary data, sending only model updates to the server. These updates are then aggregated to refine the global model. In conventional FL frameworks, the cohort of clients engaged in training is typically static, implying the objective function is also fixed.

In practical FL systems, the dynamic nature of client arrival and departure presents significant challenges to maintaining a robust and accurate model. For instance, clients may lose interest when their local data no longer aligns with the central task, such as when a user’s application shifts from text predictions to image recognition. On the other hand, clients may join when their current objectives align with those of other clients, such as when multiple users are working with similar data types or models addressing the same problem, like medical institutions collaborating on disease detection models. Additional factors, such as evolving privacy policies, or shifts in data-sharing preferences, further exacerbate these arrival and departure fluctuations, complicating the overall learning process.

Challenges: This dynamic FL setting introduces new challenges that are not present in traditional static FL scenarios with a fixed objective function. Specifically, the arrival and departure of clients dynamically alter the FL system’s objective, as the model must adapt to the current set of clients and their associated tasks. For instance, if a client contributing unique data classes withdraws, the model no longer needs to classify those classes, fundamentally altering the training objective. Conversely, the addition of clients with previously unrepresented classes necessitates model adaptation to incorporate the updated classification task. Thus, the core challenge is not merely preserving the diversity of the training set but dynamically adjusting the model to align with the evolving tasks defined by the current clients in the system. To address these shifting objectives, FL systems must be designed with the capacity for rapid and continuous adaptation, ensuring the model remains relevant, stable, and effective as the landscape of participating clients evolves.

Illustrative Examples: Figure 1 illustrates our system model, highlighting its key differences from traditional FL with partial client participation. In traditional FL with partial client participation, although the set of active clients may change as some clients intermittently disengage, the optimization goal remain constant throughout the training process. The objective is to converge towards the optimal model w^* , which minimizes the aggregated loss functions across all clients, expressed as $F_1(w) + F_2(w) + F_3(w)$. In contrast, our approach addresses a more intricate scenario where both the set of clients and the optimization goals evolve dynamically. In each round g , the set of clients changes, and the objective shifts to finding the round-specific optimal model $w^{(g)*}$, defined as the minimizer of the loss function $F_k(w)$ corresponding to the clients in that round. This dual dynamic creates substantial complexity, necessitating continuous adjustment of the optimization target to reflect the evolving composition of clients, thereby introducing challenges far beyond those encountered in traditional FL settings.

Contributions: Given the challenges introduced by the dynamic nature of client arrival and departure, this work makes the following key contributions to advance the field:

- We first propose a comprehensive probabilistic framework that models the formation of local datasets and classifies clients into distinct types based on their underlying probability distributions. This framework sheds light on the dynamics of how the optimal point shifts across global iterations, offering a detailed view of the impact of client variability on model performance. By examining the probabilistic relationships among client types and their associated data distributions, our approach highlights how changes in local datasets influence global optimization.
- We provide a novel theoretical analysis where an upper bound on the optimality gap is derived, quantifying the discrepancy between the global model and the theoretical optimal point. Our

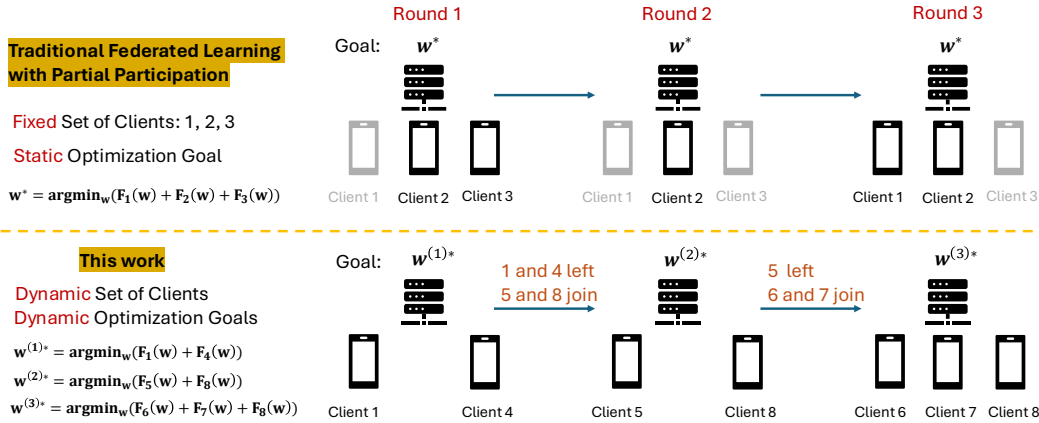


Figure 1: Comparison between traditional FL with partial participation settings and our setup. We consider both dynamic set of clients and dynamic optimization goals. In each round, our goal is to obtain a model that optimizes the loss functions of current clients. In comparison, traditional FL with partial participation approaches consider a fixed set of clients in the system with a static optimization goal as the goal is still to satisfy the clients within the current, and fixed system. Note that traditional FL with full participation is a special case of traditional FL partial participation.

analysis considers a dynamic optimization goal, where each round aims to find an optimized model that minimizes the loss function of the currently active clients, in contrast to existing literature that focuses on a static goal of minimizing the loss across all clients that have ever participated. This bound incorporates several critical factors influencing performance, including: (1) stochastic gradient noise arising from inherent randomness in local updates, (2) the number of local training iterations, which affects convergence behavior, (3) the non-IIDness of data distribution, and (4) the deviations between optimal points caused by the dynamic arrival and departure of clients. This comprehensive analysis provides a clearer understanding of the trade-offs involved in model training.

- We develop a robust algorithm for constructing an effective initial point for each training round, enabling rapid adaptation. Our approach constructs the initial model as a weighted average of previous models, with weights proportional to the similarity between the computed gradients of the models and the current set of participating clients. Leveraging these gradient-based similarities, the algorithm prioritizes models trained on clients whose data characteristics align with those of current participants, enhancing swift adaptation and mitigating performance degradation caused by dynamic client arrivals or departures. Experimental evaluations across multiple datasets demonstrate that our method achieves significant performance gains, particularly in scenarios characterized by sporadic or moderate patterns of client participation, highlighting its applicability in real-world settings.

2 RELATED WORK

Federated learning (FL) has emerged as a prominent paradigm for distributed machine learning, enabling the collaborative training of models across decentralized data sources while preserving data privacy (McMahan et al., 2017; Kairouz et al., 2019; Li et al., 2020). One of the foundational works introduced the Federated Averaging (FedAvg) algorithm, which remains a cornerstone of many FL systems (McMahan et al., 2017). Subsequent studies have explored various aspects of federated learning, including communication efficiency (Yang et al., 2019), robustness to adversarial attacks (Bagdasaryan et al., 2020), and personalization strategies (Smith et al., 2017). However, these approaches typically assume a fixed set of participating clients throughout the training process. Reviews of FL techniques often consider static client participation, where all clients are expected to remain available for the entire training duration (Kairouz et al., 2019; Li et al., 2020). This assumption simplifies the modeling of convergence and performance but does not adequately capture real-world scenarios characterized by dynamic client pattern. Addressing the dynamic nature of

client arrival and departure is a critical gap in the current literature, motivating the need for adaptive methods that can effectively handle the entry and exit of clients during the training process.

To address the limitations of static client sets in federated learning, research on dynamic client selection and flexible participation has gained momentum, particularly in response to the challenges posed by varying client availability (Fu et al., 2023; Nishio & Yonetani, 2019; Yoshida et al., 2020; AbdulRahman et al., 2020; Martini, 2024; Li et al., 2021; Lin et al., 2021; Chai et al., 2020; Gu et al., 2021; Jhunjhunwala et al., 2022). These studies explore strategies such as optimizing client selection based on resource constraints, modeling participation patterns probabilistically, and employing adaptive algorithms to address the effects of non-IID data. The goal is to enhance overall model performance by strategically managing client participation during training, balancing computational efficiency, communication costs, and data representativeness. However, these works often assume a fixed client set, neglecting the dynamic nature of client arrival and departure. While (Ruan et al., 2021a) propose a flexible federated learning framework that allows for inactive clients, incomplete updates, or dynamic client participation, their analysis is limited to scenarios where the optimization goal changes only once, specifically when a single client joins during training. This restricts the applicability of their approach to more complex and realistic patterns of client pattern.

In contrast to previous works, our approach addresses the challenge of a dynamically changing optimization goal that evolves across global rounds, focusing on the more stringent issue of dynamic client arrival and departure over time. We introduce a probabilistic framework to model the formation of local datasets, incorporating the concept of client types. These client types are characterized by the underlying probability distributions that dictate how local datasets are sampled from the global dataset. To mitigate the performance degradation caused by dynamic client arrival and departure, we propose an adaptive method for constructing the initial model. This adaptive strategy ensures robust performance, even as clients dynamically join or leave the system, leading to varying data distributions throughout training. By addressing these complexities, our framework provides a more flexible and resilient solution for federated learning in dynamic environments.

3 DYNAMIC FL WITH CLIENT ARRIVAL AND DEPARTURE

We consider a dynamic FL system where clients may join or leave the training process based on their interest or task needs. Clients may join when the model aligns with their objectives, when they have sufficient new data to contribute, or when the system offers financial or computational incentives. Conversely, they may leave if the global model drifts from their needs, if they lack sufficient data, or if the model’s performance is not beneficial. Privacy or security concerns, such as adversarial threats or inadequate privacy guarantees, may also lead clients to leave. Additionally, clients may leave to allocate computational resources to other tasks or due to poor local model validation, while others may rejoin when they see improvements in these factors.

To mathematically characterize these scenarios, each round of FL training, denoted by $g \in \mathbb{G} = \{1, \dots, G\}$, involves a set of clients collected in $\mathbb{K}^{(g)} = \{1, \dots, K^{(g)}\}$. All clients are connected to a central server, with each client maintaining its own ML models tailored to specific tasks such as pattern recognition and natural language processing. These models are trained locally on client-specific data, allowing the system to leverage diverse data sources while preserving user privacy.

Probabilistic Modeling and Definitions of Loss Functions: To gain insights into dataset randomness and quantify data heterogeneity, we develop a probabilistic model for client types and the formation of local datasets. In this model, each local dataset $\mathbb{D}_k^{(g)}$ is considered to be sampled from a universal dataset \mathbb{D} . This universal dataset represents the complete set of data that could potentially be encountered throughout all training rounds. We will further quantify this probabilistic modeling in Section 4 when we present our performance analysis. The global dataset $\mathbb{D}^{(g)}$ at any training round g is defined as the union of all local datasets $\mathbb{D}_k^{(g)}$ from clients $k \in \mathbb{K}^{(g)}$: $\mathbb{D}^{(g)} = \cup_{k \in \mathbb{K}^{(g)}} \mathbb{D}_k^{(g)}$. Based on this model, the local loss function of client k is defined as

$$F_k^{(g)}(\mathbf{w}, \mathbb{D}_k^{(g)}) \triangleq \frac{\sum_{d \in \mathbb{D}} \ell(\mathbf{w}, d) \times \mathbf{1}_{\mathbb{D}_k^{(g)}}(d)}{\sum_{d \in \mathbb{D}} \mathbf{1}_{\mathbb{D}_k^{(g)}}(d)} \triangleq \frac{\sum_{d \in \mathbb{D}} \ell(\mathbf{w}, d) \times \mathbf{1}_{\mathbb{D}_k^{(g)}}(d)}{D_k^{(g)}}. \quad (1)$$

Here, $D_k^{(g)} \triangleq \sum_{d \in \mathbb{D}} \mathbf{1}_{\mathbb{D}_k^{(g)}}(d)$ is the size of local dataset $\mathbb{D}_k^{(g)}$, $\ell(\mathbf{w}, d)$ measures the loss of data point d in universal dataset \mathbb{D} under model parameter \mathbf{w} , and finally $\mathbf{1}_{\mathbb{D}_k^{(g)}}(d)$ is the indicator function whose value is 1 if the data point d in the universal dataset belongs to the local dataset $\mathbb{D}_k^{(g)}$ and 0 otherwise. Similarly, let $D^{(g)} \triangleq \sum_{d \in \mathbb{D}} \mathbf{1}_{\mathbb{D}^{(g)}}(d)$ denote the size of global dataset $\mathbb{D}^{(g)}$, we can define the global loss function as

$$F^{(g)}(\mathbf{w}, \mathbb{D}^{(g)}) \triangleq \frac{\sum_{d \in \mathbb{D}} \ell(\mathbf{w}, d) \times \mathbf{1}_{\mathbb{D}^{(g)}}(d)}{\sum_{d \in \mathbb{D}} \mathbf{1}_{\mathbb{D}^{(g)}}(d)} = \frac{\sum_{d \in \mathbb{D}} \ell(\mathbf{w}, d) \times \mathbf{1}_{\mathbb{D}^{(g)}}(d)}{D^{(g)}}. \quad (2)$$

Local Model Training and Global Model Update: In each round of training, the server first transmits the current global model $\mathbf{w}^{(g)} \in \mathbb{R}^M$ to all clients in the current round. After receiving the global model, each client $k \in \mathbb{K}^{(g)}$ updates the model with its local dataset $\mathbb{D}_k^{(g)}$ by $e_i^{(g)}$ steps of stochastic gradient descent (SGD). At SGD iteration $h \in \{0, \dots, e_i^{(g)} - 1\}$, the update is $\mathbf{w}_k^{(g), h+1} = \mathbf{w}_k^{(g), h} - \eta^{(g)} \nabla F_k^{(g)}(\mathbf{w}_k^{(g), h}, \mathbb{B}_k^{(g)})$ where $\eta^{(g)}$ is the learning rate in g -th round, $\nabla F_k^{(g)}(\mathbf{w}_k^{(g), h}, \mathbb{B}_k^{(g)})$ is the gradient of client k 's local loss function in g -th round, $\mathbb{B}_k^{(g)} \subset \mathbb{D}_k^{(g)}$ is the mini-batch dataset drawn from the local dataset $\mathbb{D}_k^{(g)}$ to compute the stochastic gradient. Note that the initial point for the local model training is the current global model, i.e. $\mathbf{w}_k^{(g), 0} = \mathbf{w}^{(g)}$ and we denote the final local model as $\mathbf{w}_k^{(g), F}$. The primary objective of training an ML model is to minimize the global loss function, which directly affects the model's performance in real-time downstream tasks on clients. Dynamic client participation, where clients can join or leave the system at any time, causes the global loss functions to vary over time. Thus, the optimal global model parameters form a sequence $\{\mathbf{w}^{(g)*}\}_{g=1}^G$ where $\mathbf{w}^{(g)*} = \arg \min_{\mathbf{w} \in \mathbb{R}^M} F^{(g)}(\mathbf{w}, \mathbb{D}^{(g)})$, $g \in \mathbb{G}$.

Toward this goal, after all clients finish the local model training, the server sends final model $\mathbf{w}_k^{(g), F}$ to the server, which aggregate all the final global models to update the global model in the following way: $\mathbf{w}^{(g+1)} = \sum_{k \in \mathbb{K}^{(g)}} \frac{D_k^{(g)} \mathbf{w}_k^{(g), F}}{D^{(g)}}$. The server initiates the next training round by sending the updated global model $\mathbf{w}^{(g+1)}$ to the current set of clients $\mathbb{K}^{(g+1)}$, which includes clients that joined before model aggregation and excludes those that left during the previous round. Unlike existing literature that aims to minimize the loss function across all potential clients, this work focuses on optimizing for the current set of participating clients, targeting $\mathbf{w}^{(g)*}$ at each global iteration g . This approach better reflects the dynamic nature of client participation, as it avoids optimizing for clients that may not rejoin the system. In our model, existing clients must complete local training before leaving, while new clients can join at any time and will participate in the next global iteration if they join after the model broadcast.

4 CONVERGENCE ANALYSIS

In this section, we derive a convergence bound for federated learning that accounts for dynamic client participation, including both arrivals and departures. Our analysis addresses several key factors: (1) stochastic gradient noise, which arises from the inherent randomness of local updates; (2) the impact of the number of local training iterations on convergence behavior; (3) the non-IID nature of data distribution; and (4) deviations from optimal solutions due to the dynamic nature of client participation. This analysis is grounded in widely accepted assumptions (Li et al., 2019; Ruan et al., 2021b) and is framed within a probabilistic model where client types are determined by a probability distribution, which governs the random sampling process of the local dataset from the universal dataset. Our experiments include extensive tests to demonstrate that the algorithm remains robust, even when certain assumptions are not fully met.

Definition 1 (Client Type). Let \mathcal{Q} denote the set of probability distributions according to which global data are sampled and stored by the clients. For each client $k \in \mathbb{K}$, there exists a distribution $q \in \mathcal{Q}$ such that the probability that a local data sample $\mathbf{x}_k \in \mathbb{D}_k^{(g)}$ equals the global data sample $d \in \mathbb{D}^{(g)}$ is $p(\mathbf{x}_k = d) = q(d)$. Further, suppose there exists a set $\mathcal{S} \subset \mathbb{Z}^+$ that indexes these distributions so that $\mathcal{Q} = \{q_\alpha : \alpha \in \mathcal{S}\}$. We say client k is of type α if the distribution of its local samples $\mathbf{x}_k \in \mathbb{D}_k^{(g)}$ is $p(\mathbf{x}_k = d) = q_\alpha(d)$.

Assumption 1 (Finite Device Type). The number of client types $S := |\mathcal{S}|$ is finite.

Definition 2 (Mapping from client Index to client Type). For each client $k \in \mathbb{K}$, we let $\tau(k) \in \{1, 2, \dots, S\}$ denote the type of client k .

Assumption 2 (μ -Strong Convexity and L -Smoothness). All local loss functions $F_k^{(g)}$ and the global loss function $F^{(g)}$ are μ -strongly convex and L -smooth (or L -Lipschitz continuous gradient).

Definition 3 (Non-IIDness Measure). Let $\mathbf{w}^{(g)*}$ be the minimizer of $F^{(g)}$ and $\mathbf{w}_k^{(g)*}$ be the minimizer of $F_k^{(g)}$. We can quantify the heterogeneity between the data distribution of each client and that of other clients by $\Gamma_k^{(g)} = F^{(g)}(\mathbf{w}_k^{(g)*}) - F_k^{(g)}(\mathbf{w}_k^{(g)*})$.

Assumption 3 (Bounded Variance of Stochastic Gradient). Let $\nabla F_k^{(g)}(\mathbf{w}, \xi)$ be the stochastic gradient at client k in round g given parameter \mathbf{w} and a mini-batch ξ . The variance of the stochastic gradient is bounded by σ_k^2 if $\mathbb{E}_\xi \left[\|\nabla F_k^{(g)}(\mathbf{w}, \xi) - \nabla F_k^{(g)}(\mathbf{w})\|^2 \right] \leq \sigma_k^2$.

Before presenting the main analytical results, it is crucial to lay the groundwork with one lemma, which will provide the essential context and foundation needed to fully comprehend and derive the final outcomes. This lemma illustrates the maximum impact that variations in the set of clients—including the types of new clients that join the system and the types of clients that left—can have on shifting the new optimal point away from the previous optimal point.

Lemma 1. Let $\mathbf{w}^{(g)*}$ be the minimizer of $F^{(g)}$ and $\mathbf{w}^{(g+1)*}$ be the minimizer of $F^{(g+1)}$. If for all clients $k \in \mathbb{K}^{(g)}$, all rounds $g \in \mathbb{G}$, all model parameters $\mathbf{w} \in \mathbb{R}^M$, and all data $d \in \mathbb{D}$, the gradient of the loss function $\nabla \ell$ is bounded on a compact set Ω which contains the possible values of the gradient during model training, i.e. $\|\nabla \ell(\mathbf{w}, d)\| \leq C$, $\forall \mathbf{w} \in \Omega$, the expected difference between two minimizers of consecutive global loss functions is bounded as follows

$$\mathbb{E}\|\mathbf{w}^{(g)*} - \mathbf{w}^{(g+1)*}\| \leq \frac{1}{\mu} \left(\sqrt{\frac{C\pi}{12D^{(g)}}} + \sqrt{\frac{C\pi}{12D^{(g+1)}}} \right) + \frac{C}{\mu} \left| \sum_{d \in \mathbb{D}} \min\{\psi^{(g,g+1)}(d), \psi^{(g+1,g)}(d)\} \right| \quad (3)$$

where $\psi^{(g_1, g_2)}(d)$ for any $g_1 \in \mathbb{G}$ and $g_2 \in \mathbb{G}$, $g_1 \neq g_2$ is defined as follows

$$\psi^{(g_1, g_2)}(d) = \frac{\sum_{k \in \mathbb{K}^{(g_1)}} q_{\tau(i)}(d)}{D^{(g_1)}} - \frac{\sum_{i, j \in \mathbb{K}^{(g_2)}, i \neq j} q_{\tau(i)}(d)q_{\tau(j)}(d) + \sum_{k \in \mathbb{K}^{(g_2)}} q_{\tau(i)}(d)}{D^{(g_2)}} \quad (4)$$

Proof: Please see Appendix A. \square

As observed in equation 3 and equation 4, the deviation of the new optimal point $\mathbf{w}^{(g+1)*}$ from the previous one $\mathbf{w}^{(g)*}$ depends solely on the conditions in rounds g and $g + 1$. Specifically, it is influenced by factors such as the size of the local datasets for each client, the types of clients involved, and the convexity of the global function. Notably, this deviation is independent of learning parameters such as the learning rate.

To mathematically understand the performance of our machine learning algorithm in our probabilistic framework, we need to quantify how far the model at any given training round is away from the optimal point given the client pattern dynamics. We capture this by deriving an upper bound on the optimality gap which is defined to be $\|\mathbf{w}^{(g)} - \mathbf{w}^{(g)*}\|$ in a recursive relationship.

Theorem 1. If for all clients $k \in \mathbb{K}^{(g)}$, all rounds $g \in \mathbb{G}$, all model parameters $\mathbf{w} \in \mathbb{R}^M$, and all data $d \in \mathbb{D}$, the gradient of the loss function $\nabla \ell$ is bounded on a compact set Ω which contains the possible values of the gradient during model training, i.e. $\|\nabla \ell(\mathbf{w}, d)\| \leq C$, $\forall \mathbf{w} \in \Omega$, then we have the following recursive relationship between two consecutive optimality gap

$$\begin{aligned} \mathbb{E}\|\mathbf{w}^{(g+1)} - \mathbf{w}^{(g+1)*}\| &\leq 2 \underbrace{\left(1 - \frac{1}{2}\mu\eta^{(g)} \left(\sum_{k \in \mathbb{K}^{(g)}} \frac{D_k^{(g)} e_k^{(g)}}{D^{(g)}} \right) \right)}_{(a)} \mathbb{E}\|\mathbf{w}^{(g)} - \mathbf{w}^{(g)*}\| \\ &+ \underbrace{(2 + \mu\eta^{(g)}) C^2 \left(\sum_{k \in \mathbb{K}^{(g)}} \frac{D_k^{(g)} e_k^{(g)}}{D^{(g)}} \right)}_{(b)} \underbrace{\sum_{k \in \mathbb{K}^{(g)}} \frac{D_k^{(g)}}{D^{(g)}} \left(e_k^{(g)} - 1 \right) \frac{e_k^{(g)} (2e_k^{(g)} - 1)}{3}}_{(c)} + \underbrace{2\eta^{(g)} \sum_{k \in \mathbb{K}^{(g)}} \frac{D_k^{(g)} (e_k^{(g)})^2 \sigma_k^2}{D^{(g)}}}_{(c)} \\ &+ \underbrace{2\eta^{(g)} \left(\sum_{k \in \mathbb{K}^{(g)}} \frac{D_k^{(g)} (L\eta^{(g)} e_k^{(g)} + 2L\eta^{(g)} + 1) e_k^{(g)}}{D^{(g)}} \mathbb{E}[\Gamma_k^{(g)}] \right)}_{(d)} + \underbrace{\frac{2}{\mu} \left(\sqrt{\frac{C\pi}{12D^{(g)}}} + \sqrt{\frac{C\pi}{12D^{(g+1)}}} \right) + \frac{2C}{\mu} \left| \sum_{d \in \mathbb{D}} \min\{\psi^{(g,g+1)}(d), \psi^{(g+1,g)}(d)\} \right|}_{(e)} \end{aligned} \quad (5)$$

Proof: Please see Appendix B. □

For any client participation pattern, regardless of how many clients join or leave the system, equation 5 captures the impact of heterogeneity on the ML performance by detailing: (1) the number of local SGD iterations $e_k^{(g)}$, (2) the non-IIDness of each client $\Gamma_k^{(g)}$, (3) local SGD noises σ_k , and (4) the size of local dataset and the types of each client in dynamic FL scenarios.

In the following, we examine each term in equation 5. Term (a) establishes the recursive relationship and explicitly identifies the factors influencing the contraction coefficient $1 - (1/2)\mu\eta^{(g)}(\sum_{k \in \mathbb{K}^{(g)}} (D_k^{(g)} e_k^{(g)} / D^{(g)}))$. A larger strong convexity coefficient μ , an increased number of local SGD iterations $e_k^{(g)}$ and a higher learning rate $\eta_k^{(g)}$ all contribute to a smaller contraction coefficient. To expand this recursive relationship from the initial point, relating the optimality gap between round $g + 1$ and round 0, it is crucial to select an appropriate learning rate $\eta^{(g)}$ to ensure convergence. The contraction coefficient must be kept between 0 and 1 to guarantee that the sequence converges. Term (b) illustrates the influence of the number of local SGD iterations $e_k^{(g)}$ and the gradient bounding constant C of the gradient. Notably, when each client performs only one local SGD (i.e. $e_k^{(g)} = 1$), the bounding constant C does not affect the bound. Term (c) indicates that clients with larger SGD noise σ_k will see a greater deviation of the model from the current optimal point when performing more local SGD iterations $e_k^{(g)}$. It is particularly concerning that the SGD noise accumulates with the square of the number of local SGD iterations, resulting in a more rapid increase in deviation. This effect is further intensified with a larger local dataset size. Term (d) highlights the impact of the non-IIDness metric $\Gamma_k^{(g)}$ and its interaction with the number of local SGD iterations. For clients with larger $\Gamma_k^{(g)}$, performing more local SGD iterations biases the local model toward the local dataset, thereby compromising the performance of the global model when aggregated. Additionally, if the function's gradient is not smooth (i.e., if the smoothness constant L is large), the non-IIDness metric will have a more pronounced effect on the optimality gap. Finally, term (e) represents the expected difference between two optimizers $\mathbf{w}^{(g)*}$ and $\mathbf{w}^{(g+1)*}$. As shown in Lemma 1, several factors can lead to a larger difference, thereby increasing the optimality gap in round $g + 1$. These factors include (1) the types of new clients joining the system, (2) the types of clients leaving, (3) the size of the global dataset in rounds g and $g + 1$, and (4) the sizes of the local datasets of the joining and leaving clients.

5 DYNAMIC INITIAL MODEL CONSTRUCTION FOR FAST ADAPTATION

Algorithm 1 FederatedTraining($\mathbf{w}_{\text{init}}, \mathbb{K}^{(g)}, \{e_k^{(g)}\}, V$)

Input: Number of global rounds V , a initial global model \mathbf{w}_{init} , set of clients $\mathbb{K}^{(g)}$ in each global round, number of local epochs $e_k^{(g)}$ for each client k .

- 1: **for** $v = 0, \dots, V - 1$ **do**
- 2: **if** $v == 0$ **then** $\mathbf{w}^{(v)} \leftarrow \mathbf{w}_{\text{init}}$
- 3: **for** $k \in \mathbb{K}^{(g)}$ **do**
- 4: **for** $h \in \{0, \dots, e_k^{(g)} - 1\}$ **do** Perform local model training based on $\mathbf{w}^{(v)}$
- 5: Send the final local model $\mathbf{w}_k^{(v),F}$ to the server
- 6: The server performs aggregation using weighted summation to get $\mathbf{w}^{(v+1)}$.
- 7: **return** $\mathbf{w}^{(V-1)}$

Motivation: Although our analysis applies to any client pattern, machine learning performance can be further improved by utilizing historical data distributions. Intuitively, if the data distribution in round g closely resembles that of a previous round g' , where $g' < g$, initializing the global model in round g with the model from round g' can lead to significant performance gains. This approach leverages past knowledge to accelerate convergence and mitigates the adverse effects of sporadic or unpredictable client patterns, which often cause fluctuations in model quality. By reusing model states from rounds with similar data distributions, the learning process becomes more robust, reducing the need for the model to relearn from scratch when encountering familiar data patterns.

Algorithm 2 Dynamic Initial Model Construction for Fast Adaptation

Input: The number of global rounds within one session T , the number of sessions in pilot model preparation stage P , the number of sessions to execute $S(\geq P)$, the number of global rounds V to compute the gradient used to calculate similarity, and a similarity scaling factor R .

- 1: **Initialize:** Randomly initialize global model $\mathbf{w}^{(0)}$
- 2: **for** $g = 0, \dots, ST - 1$ **do**
- 3: **if** at the beginning of each session after pilot preparation stage **then**
- 4: $\mathbf{w}_{\text{Pilot}}^{(V-1)} \leftarrow \text{FederatedTraining}(\mathbf{w}_{\text{Pilot}}, \mathbb{K}^{(g)}, \{e_k^{(g)}\}, V)$
- 5: $\nabla F_{\text{Pilot}}^g \leftarrow \mathbf{w}_{\text{Pilot}}^{(V-1)} - \mathbf{w}_{\text{Pilot}}$
- 6: **if** at least one gradient computed based on $\mathbf{w}_{\text{Pilot}}$ in the past **then**
- 7:
$$\mathbf{w}^{(g)} \leftarrow \sum_{s=P}^{\lfloor g/T \rfloor - 1} \left(\frac{\exp(-R\|\nabla F_{\text{Pilot}}^s - \nabla F_{\text{Pilot}}^g\|_2)}{\sum_{s=P}^{\lfloor g/T \rfloor - 1} \exp(-R\|\nabla F_{\text{Pilot}}^s - \nabla F_{\text{Pilot}}^g\|_2)} \times \mathbf{w}^{(s)} \right)$$
- 8: Save $\nabla F_{\text{Pilot}}^g$
- 9: $\mathbf{w}^{(g+1)} \leftarrow \text{FederatedTraining}(\mathbf{w}^{(g)}, \mathbb{K}^{(g)}, \{e_k^{(g)}\}, 1)$
- 10: **if** the final global round in each session **then** Save $\mathbf{w}^{(g+1)}$
- 11: **if** there are P saved models (i.e. pilot preparation stage ends) **then**
- 12: Exclude models that do not have good accuracy
- 13: The pilot model $\mathbf{w}_{\text{Pilot}} \leftarrow$ The average of all remaining models

Intuition: In complex scenarios, where data distributions are heterogeneous or where no data distribution resembles the current one, it is more advantageous to initialize the model using a weighted sum of models from multiple prior rounds. The weight assigned to each model should ideally reflect the degree of similarity between data distributions in a past round g' and the current round g . However, systematically calculating this similarity and determining the appropriate weights remains a challenging task. To address this, we propose utilizing a “pilot model” to compute gradients, which are then employed to assess similarity and derive the weights for the weighted sum.

Federated Training (Algorithm 1): Algorithm 1 outlines the federated learning procedure, which serves as a key component of our main algorithm. It takes several inputs: the number of global rounds V , an initial global model \mathbf{w}_{init} , the set of clients $\mathbb{K}^{(g)}$ in each global round, and the number of local epochs $e_k^{(g)}$ for each client k . Based on these inputs, Algorithm 1 performs federated training, yielding the final global model $\mathbf{w}^{(V-1)}$ after V global rounds. Moreover, Algorithm 1 is adaptable to different federated learning variants by adjusting the local training process and the global model aggregation method, thereby extending the applicability of our proposed algorithm.

Dynamic Initial Model Construction for Fast Adaptation (Algorithm 2): The algorithm begins with a randomly initialized model $\mathbf{w}^{(0)}$ (Line 1) and applies Algorithm 1 (Line 9) using the current global model $\mathbf{w}^{(g)}$ as the initial model, performing one global round to update it. If the global round is the last in a session (Line 10), the global models are saved for constructing both the pilot and dynamic initial models later. Upon completing the predefined P sessions in the pilot preparation stage (Line 11), the pilot model $\mathbf{w}_{\text{Pilot}}$ is formed by averaging the global models with good accuracy, as models with poor accuracy do not effectively capture the underlying data distribution. Importantly, the pilot model is computed only once during the algorithm’s entire execution. After the pilot preparation stage, at the start of each subsequent session (Line 3), Algorithm 1 is executed with V global rounds, using $\mathbf{w}_{\text{Pilot}}$ as the initial global model to obtain $\mathbf{w}_{\text{Pilot}}^{(V-1)}$ (Line 4). The difference between the updated global model $\mathbf{w}_{\text{Pilot}}^{(V-1)}$ and the pilot model $\mathbf{w}_{\text{Pilot}}$ yields the gradient $\nabla F_{\text{Pilot}}^g$ (Line 5), which characterizes the current data distribution. These gradients are saved to compute similarity between data distributions (Line 8). If at least one past gradient exists (Line 6), the initial model is constructed using a weighted sum of all saved models after the pilot preparation stage (Line 7). The weight assigned to each model is proportional to the similarity between the current gradient $\nabla F_{\text{Pilot}}^g$ and a past gradient $\nabla F_{\text{Pilot}}^s$, quantified by the negative two-norm of their difference, $-\|\nabla F_{\text{Pilot}}^s - \nabla F_{\text{Pilot}}^g\|_2$. A scaling factor R adjusts the sensitivity of the similarity measure, and the `softmax` function is applied to these scaled differences, producing normalized weights that sum to one. The closer the gradients, the smaller the two-norm, and consequently, the higher the weight. This ensures that the initial model emphasizes models with gradients that closely match those of

the current clients, enabling rapid adaptation and minimizing performance loss due to the dynamic nature of client participation. By tuning R , the construction of the initial model can be controlled. When $R = 0$, the model becomes an average of all saved models after the pilot preparation stage, regardless of data distribution similarity. As $R \rightarrow \infty$, the initial model becomes the saved model trained on the data distribution most similar to the current one.

6 EXPERIMENTS

FL Algorithm and Baseline: We consider FedAvg and FedProx (Li et al., 2020) as the federated learning algorithms used in our experiments to evaluate proposed algorithm. For both FedAvg and FedProx, the baseline continues model training using the previous model from the last round, without constructing an appropriate initial model.

Task and Dataset: We conducted extensive experiments to evaluate Algorithm 2. The task of interest is image classification. We used five image datasets, ranging from simple to the most challenging: MNIST (LeCun et al., 1998), Fashion-MNIST (Xiao et al., 2017), SVHN (Netzer et al., 2011), CIFAR10 (Krizhevsky & Hinton, 2009), and CIFAR100 (Krizhevsky & Hinton, 2009). CIFAR100 contains 100 labels, while the others have 10 labels each. The models for MNIST, Fashion-MNIST, and SVHN are outlined in Appendix C.2. Specifically, the models for MNIST and Fashion-MNIST are simple multi-layer perceptrons (MLP), while the model for SVHN is a convolutional neural network (CNN). For CIFAR10 and CIFAR100, we used the ResNet18 architecture (He et al., 2016).

Label Distribution: In our experiments, we simulate a system of 10 clients. We consider four methods for distributing the labels across these clients:

- **Two-Shard**(McMahan et al., 2017; Hsu et al., 2019; Li et al., 2020; Fallah et al., 2020; Karimireddy et al., 2020): For datasets with 10 labels, each label is divided into two equally-sized shards, and each client receives two different label shards. For datasets with 100 labels, the labels are divided into 10 non-overlapping batches, and each batch is split into two shards, which are then assigned to two randomly selected clients. Each client ends up with data from two labels for 10-label datasets, or 20 labels for 100-label datasets .
- **Half:** Half the clients have one half of the labels, and the rest have the other half. Each client has all the labels from their assigned half (i.e., 5 labels for 10-label datasets or 50 labels for 100-label datasets), and the data is evenly distributed, meaning that the amount of data for each label is equally divided among the clients.
- **Partial-Overlap:** Two sets of labels are selected, each containing 60% of the total labels, with a 20% overlap between them. Each client in the first set has 6 labels for 10-label datasets (or 60 labels for 100-label datasets), and each client in the second set has a similar distribution. The overlapping labels are split between the two halves of clients, with half of the data for overlapping labels going to the first set of clients and the other half to the second set. The non-overlapping labels are assigned to the clients within each set, and the data corresponding to these labels is evenly distributed across the clients, meaning that each client receives an approximately equal share of the data for their assigned labels.
- **Distinct:** Each client is assigned a unique set of labels. For datasets with 10 labels, each client receives 1 unique label, while for datasets with 100 labels, each client receives 10 unique labels.

Test Dataset and Client Pattern: As data distributions change across global rounds, the test dataset for each round includes data with labels that are the union of the labels held by all clients in that round. The client patterns used in all experiments are provided in Appendix C.

Results and Takeaways: Table 1 presents a comparative analysis of the average accuracy of proposed algorithm for both FedAvg and FedProx over the first T global rounds (with $T = 10$) following three shifts in data distribution. The results, encompassing all datasets, label distributions, and models, demonstrate that our algorithm effectively mitigates performance degradation caused by dynamic client arrivals and departures. Additionally, it accelerates performance recovery when the current data distribution closely resembles a previous one. Figure 2, which focuses on selected scenarios, further illustrates the advantages of our algorithm for both FedAvg and FedProx during periods of significant performance drops or boosts resulting from data distribution shifts. In both

FL Algorithm	Label Distribution	Dataset (Model)	1st Transition		2nd Transition		3rd Transition	
			Proposed	Baseline	Proposed	Baseline	Proposed	Baseline
FedProx	Two-Shard	MNIST (MLP)	91.71	87.88	98.45	96.4	94.77	90.72
		Fashion-MNIST (MLP)	96.82	95.32	92.04	90.31	97.59	96.38
		SVHN (CNN)	61.35	45.09	55.12	36.28	86.52	40.13
		CIFAR10 (ResNet18)	91.77	83.88	46.26	35.62	82.58	58.34
	Half	CIFAR100 (ResNet18)	49.28	46.52	63.5	62.03	52.73	48.35
		MNIST (MLP)	96.02	90.12	93.01	87.83	96.29	90.56
		Fashion-MNIST (MLP)	86.35	84.6	90.97	86.02	86.62	85.06
		SVHN (CNN)	93.37	10.89	91.45	20.41	93.51	61.84
	Partial-Overlap	CIFAR10 (ResNet18)	86.32	48.83	90.38	54.74	87.68	58.41
		CIFAR100 (ResNet18)	62.88	56.16	64.27	57.14	63.53	57.41
		MNIST (MLP)	90.92	86.23	94.09	89.7	91.32	87.35
		Fashion-MNIST (MLP)	86.44	82.75	87.74	85.02	87.06	83.79
Distinct	SVHN (CNN)	92.26	72.61	93.44	62.79	92.4	76.09	
	CIFAR10 (ResNet18)	81.5	77.05	86.99	83.88	81.69	79.8	
	CIFAR100 (ResNet18)	59.09	54.94	59.22	55.09	59.34	56.11	
	MNIST (MLP)	98.05	92.75	95.98	88.77	94.11	85.66	
FedAvg	Two-Shard	Fashion-MNIST (MLP)	95.5	92.4	95.8	90.59	94.02	87.36
		SVHN (CNN)	95.28	49.68	92.25	45.18	87.91	38.45
		MNIST (MLP)	98.45	96.4	94.77	90.72	98.56	96.53
		Fashion-MNIST (MLP)	92.04	90.31	97.59	96.38	95.39	93.54
	Half	SVHN (CNN)	54.05	32.49	83.45	39.58	95.87	42.97
		CIFAR10 (ResNet18)	92.01	86.83	42.42	34.28	91.91	89.25
		CIFAR100 (ResNet18)	49.63	46.04	63.01	61.36	52.18	48.43
		MNIST (MLP)	92.25	86.76	96.03	90.12	92.56	87.83
	Partial-Overlap	Fashion-MNIST (MLP)	89.74	85.01	86.24	84.54	90.29	86.12
		SVHN (CNN)	91.63	71.49	93.54	51.98	91.98	42.34
		CIFAR10 (ResNet18)	90.19	70.15	86.23	77.41	90.03	73.55
		CIFAR100 (ResNet18)	57.41	52.95	57.09	53.7	57.48	53.38
Distinct	MNIST (MLP)	93.81	89.65	91.11	87.46	94.16	90.1	
	Fashion-MNIST (MLP)	87.58	85.06	86.77	83.88	87.64	85.59	
	SVHN (CNN)	92.27	79.11	93.67	82.01	92.48	77.2	
	CIFAR10 (ResNet18)	85.87	82.35	79.94	77.1	85.87	82.9	
Distinct	CIFAR100 (ResNet18)	56.94	53.29	57.25	54.17	57.35	54.41	
	MNIST (MLP)	97.97	93.03	95.72	89.19	94.04	86.11	
	Fashion-MNIST (MLP)	95.38	92.64	95.81	90.66	93.88	87.5	
		SVHN (CNN)	94.99	49.88	91.9	38.94	87.21	32.71

Table 1: The average accuracy of proposed algorithm for FedProx and FedAvg over the first T global rounds (with $T = 10$) following a change in data distribution shows that our proposed scheme significantly outperforms the baseline across various label distributions, datasets, and models.

cases, the algorithm assigns higher importance to models trained on past distributions that share similarities with the current one, allowing the initial model to adapt more rapidly to the new distribution, consistently outperforming the baseline. The results confirm the effectiveness of our approach across various federated learning algorithms, datasets, models, and data distributions.

Other Experimental Results: Additional figures for other scenarios in Table 1 are included in Appendix C. These results demonstrate the broad applicability of proposed algorithm across different federated learning frameworks.

7 CONCLUSION

In this paper, we addressed the challenges of dynamic federated learning by introducing an optimization framework that adapts to dynamic client arrival and departure. Our approach accounts for these fluctuations and provides insights into how they influence shifts in optimal points. By establishing an upper bound on the optimality gap and proposing an adaptive initial model construction strategy guided by gradient similarity, we demonstrated enhanced adaptability to the current client set. Empirical results validate the robustness of our method across various datasets and dynamic client participation patterns. One promising direction for future work is to refine the initial model construction process, such that the model is only updated when beneficial or necessary, potentially reducing computational overhead while maintaining performance. This opens avenues for more efficient FL systems that can dynamically balance the trade-offs between adaptation and stability.

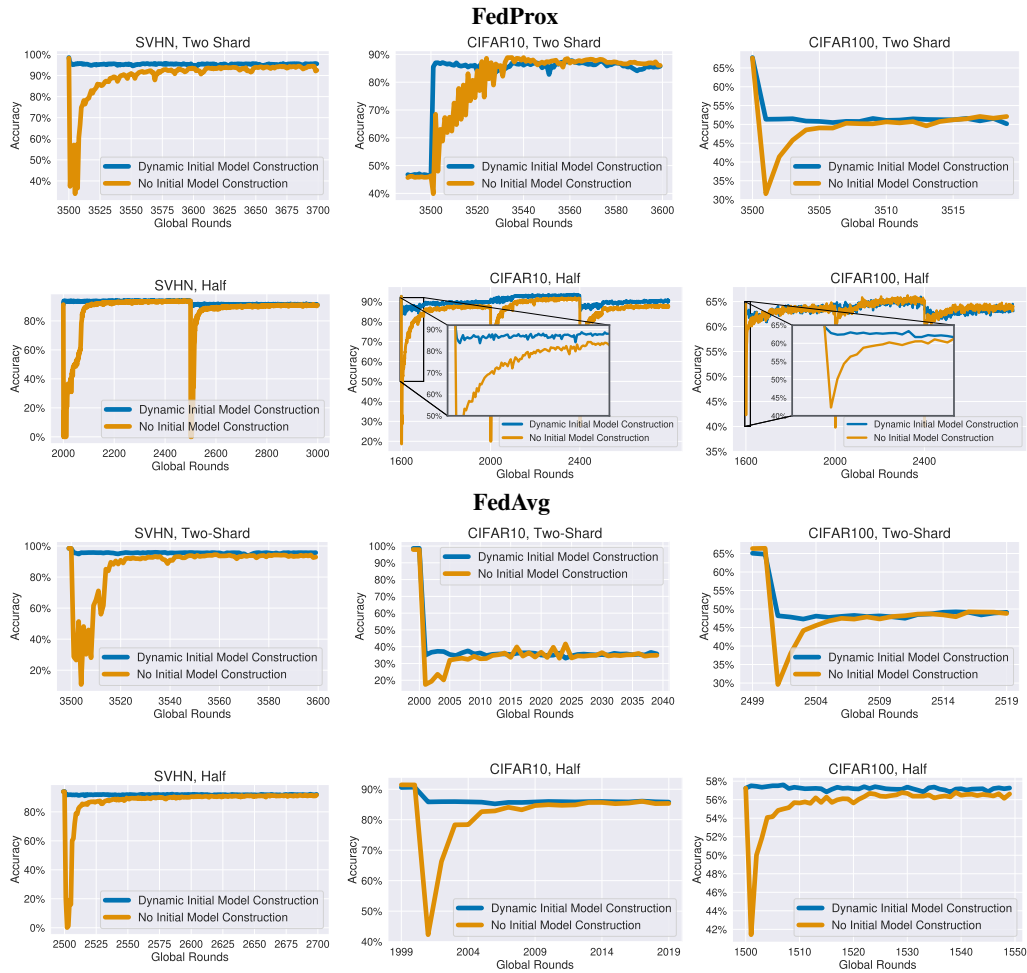


Figure 2: Performance comparison of proposed algorithm for FedProx and FedAvg with SVHN, CIFAR 10, and CIFAR 100 using Two-Shard and Half label distributions. Our proposed scheme shows robustness to the dynamic data distribution caused by dynamic client arrival and departure.

8 REPRODUCIBILITY

We utilize open-source datasets as described in Section 6. The complete mathematical proofs and details can be found in Appendix A and B. The code for training and testing is provided in the supplementary material.

REFERENCES

- Saad AbdulRahman, Hajar Tout, Amine Mourad, and Chadi Talhi. Fedmccs: Multicriteria client selection model for optimal iot federated learning. *IEEE Internet of Things Journal*, 8(6):4723–4735, 2020.
- Eugene Bagdasaryan, Andreas Veit, Yiqing Hua, Deborah Estrin, and Vitaly Shmatikov. How to backdoor federated learning. In *Proceedings of the 23rd International Conference on Artificial Intelligence and Statistics (AISTATS)*, pp. 2938–2948. PMLR, 2020.
- Lu Chai, Yongsheng Chen, Jiangfeng Cheng, Gendai Meng, Yongxin Wang, and Wei Zhang. Fedat: A high-performance federated learning system with asynchronous model update and temporally weighted aggregation. In *Proceedings of the 2020 IEEE 26th International Conference on Parallel and Distributed Systems (ICPADS)*, pp. 1081–1088. IEEE, 2020.
- Alireza Fallah, Aryan Mokhtari, and Asuman Ozdaglar. Personalized federated learning with theoretical guarantees: A model-agnostic meta-learning approach. In *Advances in Neural Information Processing Systems (NeurIPS)*, volume 33, pp. 3557–3568, 2020.
- Lei Fu, Huanle Zhang, Ge Gao, and Xin Liu. Client selection in federated learning: Principles, challenges, and opportunities. *IEEE Internet of Things Journal*, 10:1–10, 2023.
- Xinran Gu, Kaixuan Huang, Jingzhao Zhang, and Longbo Huang. Fast federated learning in the presence of arbitrary device unavailability. *Advances in Neural Information Processing Systems*, 34:12052–12064, 2021.
- Kaiming He, Xiangyu Zhang, Shaoqing Ren, and Jian Sun. Deep residual learning for image recognition. In *Proceedings of the IEEE conference on computer vision and pattern recognition*, pp. 770–778, 2016.
- Tiffany Hsu, Hang Qi, and Matthew Brown. Measuring the effects of non-identical data distribution for federated visual classification. In *Proceedings of the Workshop on Federated Learning for Data Privacy and Confidentiality (NeurIPS)*, 2019.
- Divyansh Jhunjunwala, Pranay Sharma, Aushim Nagarkatti, and Gauri Joshi. Fedvarp: Tackling the variance due to partial client participation in federated learning. In *Uncertainty in Artificial Intelligence*, pp. 906–916. PMLR, 2022.
- Peter Kairouz, H. Brendan McMahan, Brendan Avent, Aurélien Bellet, Mehdi Bennis, Arjun Nitin Bhagoji, Kallista Bonawitz, Zachary Charles, Graham Cormode, Rachel Cummings, et al. Advances and open problems in federated learning. *arXiv preprint arXiv:1912.04977*, 2019.
- Sai Praneeth Karimireddy, Satyen Kale, Mehryar Mohri, Sashank J Reddi, Sebastian U Stich, and Ananda Theertha Suresh. Scaffold: Stochastic controlled averaging for on-device federated learning. In *Proceedings of the 37th International Conference on Machine Learning (ICML)*, pp. 5132–5143, 2020.
- Alex Krizhevsky and Geoffrey Hinton. Learning multiple layers of features from tiny images. Technical report, University of Toronto, 2009.
- Yann LeCun, Léon Bottou, Yoshua Bengio, and Patrick Haffner. Gradient-based learning applied to document recognition. *Proceedings of the IEEE*, 86(11):2278–2324, 1998.
- Tian Li, Anit Kumar Sahu, Manzil Zaheer, Maziar Sanjabi, Ameet Talwalkar, and Virginia Smith. Federated optimization in heterogeneous networks. *Proceedings of Machine learning and systems*, 2:429–450, 2020.

-
- Wenhao Li, Chaohong Ding, Guangwen Zhang, and Jun Li. Model agnostic federated learning with a probabilistic client selection algorithm. In *2021 IEEE International Conference on Communications Workshops (ICC Workshops)*, pp. 1–6. IEEE, 2021.
- Xiang Li, Kaixuan Huang, Wenhao Yang, Shusen Wang, and Zhihua Zhang. On the convergence of fedavg on non-iid data. *arXiv preprint arXiv:1907.02189*, 2019.
- Tao Lin, Lingjuan Kong, Sebastian U. Stich, and Martin Jaggi. Ensemble distillation for robust model fusion in federated learning. In *Advances in Neural Information Processing Systems (NeurIPS)*, volume 34, pp. 21154–21166, 2021.
- Barbara Martini. Federated learning in dynamic and heterogeneous environments: Advantages, performances, and privacy problems. *Applied Sciences*, 14(18):8490, 2024.
- H. Brendan McMahan, Eider Moore, Daniel Ramage, Seth Hampson, and Blaise Aguera y Arcas. Communication-efficient learning of deep networks from decentralized data. In *Proceedings of the 20th International Conference on Artificial Intelligence and Statistics (AISTATS)*, pp. 1273–1282. PMLR, 2017.
- Yuval Netzer, Tao Wang, Adam Coates, Alessandro Bissacco, Bo Wu, and Andrew Y Ng. Reading digits in natural images with unsupervised feature learning. *NIPS Workshop on Deep Learning and Unsupervised Feature Learning*, 2011.
- Tadashi Nishio and Ryo Yonetani. Client selection for federated learning with heterogeneous resources in mobile edge. In *ICC 2019-2019 IEEE International Conference on Communications (ICC)*, pp. 1–7. IEEE, 2019.
- Yichen Ruan, Xiaoxi Zhang, Shu-Che Liang, and Carlee Joe-Wong. Towards flexible device participation in federated learning. In *Proceedings of The 24th International Conference on Artificial Intelligence and Statistics*, volume 130 of *Proceedings of Machine Learning Research*, pp. 3403–3411. PMLR, 2021a.
- Yichen Ruan, Xiaoxi Zhang, Shu-Che Liang, and Carlee Joe-Wong. Towards flexible device participation in federated learning. In *International Conference on Artificial Intelligence and Statistics*, pp. 3403–3411. PMLR, 2021b.
- Virginia Smith, Chao-Kai Chiang, Maziar Sanjabi, and Ameet Talwalkar. Federated multi-task learning. In *Proceedings of the 31st International Conference on Neural Information Processing Systems (NeurIPS)*, pp. 4424–4434. Curran Associates, Inc., 2017.
- Han Xiao, Kashif Rasul, and Roland Vollgraf. Fashion-mnist: a novel image dataset for benchmarking machine learning algorithms. *arXiv preprint arXiv:1708.07747*, 2017.
- Qiang Yang, Yang Liu, Tianjian Chen, and Yongxin Tong. Federated machine learning: Concept and applications. In *ACM Transactions on Intelligent Systems and Technology (TIST)*, volume 10, pp. 1–19. ACM, 2019.
- Naoki Yoshida, Tadashi Nishio, Masahiro Morikura, and Kazuaki Yamamoto. Mab-based client selection for federated learning with uncertain resources in mobile networks. In *2020 IEEE Globecom Workshops (GC Workshops)*, pp. 1–6. IEEE, 2020.

A PROOF OF LEMMA 1

I first present Hoeffding’s inequality which will be useful in our proof of Lemma 1.

Fact 1 (Hoeffding’s inequality). *Let $\{X_k\}_{k=1}^n$ be independent random variables such that $P(X_k \in [a_k, b_k]) = 1$ for some $a_k < b_k$, and let $\epsilon > 0$, $\bar{X} = \frac{1}{n} \sum_k X_k$. Then:*

$$\mathbb{P}(\|\bar{X} - \mathbb{E}[\bar{X}]\| \geq \epsilon) \leq 2 \exp\left(-\frac{12n^2\epsilon^2}{\sum_k (b_k - a_k)^2}\right) \quad (6)$$

We repeat the statement of Lemma 1 below for completeness.

Lemma 1. Let $\mathbf{w}^{(g)*}$ be the minimizer of $F^{(g)}$ and $\mathbf{w}^{(g+1)*}$ be the minimizer of $F^{(g+1)}$. If for all clients $k \in \mathbb{K}^{(g)}$, all rounds $g \in \mathbb{G}$, all model parameters $\mathbf{w} \in \mathbb{R}^M$, and all data $d \in \mathbb{D}$, the gradient of the loss function $\nabla \ell$ is bounded on a compact set Ω which contains the possible values of the gradient during model training, i.e. $\|\nabla \ell(\mathbf{w}, d)\| \leq C$, $\forall \mathbf{w} \in \Omega$, the expected difference between two minimizers of consecutive global loss functions is bounded as follows

$$\begin{aligned} \mathbb{E}\|\mathbf{w}^{(g)*} - \mathbf{w}^{(g+1)*}\| &\leq \frac{1}{\mu} \left(\sqrt{\frac{C\pi}{12D^{(g)}}} + \sqrt{\frac{C\pi}{12D^{(g+1)}}} \right) \\ &+ \frac{C}{\mu} \left| \sum_{d \in \mathbb{D}} \min\{\psi^{(g,g+1)}(d), \psi^{(g+1,g)}(d)\} \right| \end{aligned} \quad (7)$$

where $\psi^{(g_1, g_2)}(d)$ for any $g_1 \in \mathbb{G}$ and $g_2 \in \mathbb{G}$, $g_1 \neq g_2$ is defined as follows

$$\psi^{(g_1, g_2)}(d) = \frac{\sum_{k \in \mathbb{K}^{(g_1)}} q_{\tau(i)}(d)}{D^{(g_1)}} - \frac{\sum_{i, j \in \mathbb{K}^{(g_2)}, i \neq j} q_{\tau(i)}(d)q_{\tau(j)}(d) + \sum_{k \in \mathbb{K}^{(g_2)}} q_{\tau(i)}(d)}{D^{(g_2)}} \quad (8)$$

Proof: By μ -strong convexity, we have

$$\mu\|\mathbf{w}^{(g)*} - \mathbf{w}^{(g+1)*}\| \leq \|\nabla F^{(g+1)}(\mathbf{w}^{(g)*}) - \nabla F^{(g+1)}(\mathbf{w}^{(g+1)*})\| \quad (9)$$

Since $\nabla F^{(g+1)}(\mathbf{w}^{(g+1)*}) = 0 = \nabla F^{(g)}(\mathbf{w}^{(g)*})$, we have

$$\nabla F^{(g+1)}(\mathbf{w}^{(g)*}) - \nabla F^{(g+1)}(\mathbf{w}^{(g+1)*}) = \nabla F^{(g+1)}(\mathbf{w}^{(g)*}) - \nabla F^{(g)}(\mathbf{w}^{(g)*})$$

Combining all these, we will have

$$\mu\|\mathbf{w}^{(g)*} - \mathbf{w}^{(g+1)*}\| \leq \|\nabla F^{(g+1)}(\mathbf{w}^{(g)*}) - \nabla F^{(g)}(\mathbf{w}^{(g)*})\| \quad (10)$$

Based on equation 3, we have

$$\mathbb{E}\|\mathbf{w}^{(g)*} - \mathbf{w}^{(g+1)*}\| \leq \frac{1}{\mu} \mathbb{E}\|\nabla F^{(g+1)}(\mathbf{w}^{(g)*}) - \nabla F^{(g)}(\mathbf{w}^{(g)*})\| \quad (11)$$

Now, the goal is to derive an upper bound on $\mathbb{E}\|\nabla F^{(g+1)}(\mathbf{w}^{(g)*}) - \nabla F^{(g)}(\mathbf{w}^{(g)*})\|$. We have the following equality:

$$\begin{aligned} &\|\nabla F^{(g)}(\mathbf{w}) - \nabla F^{(g+1)}(\mathbf{w})\| \\ &= \|\nabla F^{(g)}(\mathbf{w}) - \mathbb{E}[\nabla F^{(g)}(\mathbf{w})] + \mathbb{E}[\nabla F^{(g)}(\mathbf{w})] - \mathbb{E}[\nabla F^{(g+1)}(\mathbf{w})] \\ &\quad + \mathbb{E}[\nabla F^{(g+1)}(\mathbf{w})] - \nabla F^{(g+1)}(\mathbf{w})\| \\ &\leq \|\nabla F^{(g)}(\mathbf{w}) - \mathbb{E}[\nabla F^{(g)}(\mathbf{w})]\| + \|\mathbb{E}[\nabla F^{(g)}(\mathbf{w})] - \mathbb{E}[\nabla F^{(g+1)}(\mathbf{w})]\| \\ &\quad + \|\mathbb{E}[\nabla F^{(g+1)}(\mathbf{w})] - \nabla F^{(g+1)}(\mathbf{w})\| \end{aligned} \quad (12)$$

Taking the expectation of both sides of equation 12 and using the fact that the middle term is already a scalar, we have:

$$\mathbb{E}\|\nabla F^{(g)}(\mathbf{w}) - \nabla F^{(g+1)}(\mathbf{w})\| \quad (13)$$

$$\leq \underbrace{\mathbb{E}\|\nabla F^{(g)}(\mathbf{w}) - \mathbb{E}[\nabla F^{(g)}(\mathbf{w})]\|}_A + \underbrace{\|\mathbb{E}[\nabla F^{(g)}(\mathbf{w})] - \mathbb{E}[\nabla F^{(g+1)}(\mathbf{w})]\|}_B \quad (14)$$

$$+ \underbrace{\mathbb{E}\|\nabla F^{(g+1)}(\mathbf{w}) - \nabla F^{(g+1)}(\mathbf{w})\|}_C \quad (15)$$

We first examine the expression for B . The expectation of the global loss function at round $g + 1$

$$\begin{aligned} \mathbb{E}[\nabla F^{(g+1)}(\mathbf{w})] &= \frac{1}{D^{(g+1)}} \sum_{d \in \mathbb{D}} \mathbb{E}[\nabla \ell(\mathbf{w}, d) \times \mathbf{1}_{\mathbb{D}^{(g+1)}}(d)] \\ &= \frac{1}{D^{(g+1)}} \sum_{d \in \mathbb{D}} \mathbb{E}[\nabla \ell(\mathbf{w}, d) \mid d \in \mathbb{D}^{(g+1)}] \times \mathbb{P}(d \in \mathbb{D}^{(g+1)}) \end{aligned} \quad (16)$$

Similarly, the expectation of the global loss function at round g

$$\begin{aligned}\mathbb{E}[\nabla F^{(g)}(\mathbf{w})] &= \frac{1}{D^{(g)}} \sum_{d \in \mathbb{D}} \mathbb{E}[\nabla \ell(\mathbf{w}, d) \times \mathbf{1}_{\mathbb{D}^{(g)}}(d)] \\ &= \frac{1}{D^{(g)}} \sum_{d \in \mathbb{D}} \mathbb{E}[\nabla \ell(\mathbf{w}, d) \mid d \in \mathbb{D}^{(g)}] \times \mathbb{P}(d \in \mathbb{D}^{(g)})\end{aligned}\quad (17)$$

The difference between the expectations is

$$\mathbb{E}[\nabla F^{(g+1)}(\mathbf{w})] - \mathbb{E}[\nabla F^{(g)}(\mathbf{w})] \quad (18)$$

$$\leq C \sum_{d \in \mathbb{D}} \left(\frac{\mathbb{P}(d \in \mathbb{D}^{(g+1)})}{D^{(g+1)}} - \frac{\mathbb{P}(d \in \mathbb{D}^{(g)})}{D^{(g)}} \right) \quad (19)$$

$$\leq C \sum_{d \in \mathbb{D}} \underbrace{\left(\frac{D^{(g)} \mathbb{P}(d \in \mathbb{D}^{(g+1)}) - D^{(g+1)} \mathbb{P}(d \in \mathbb{D}^{(g)})}{D^{(g+1)} D^{(g)}} \right)}_{B_1} \quad (20)$$

Now, we should derive an upper bound on B_1 . We assume that there is only a total of K types of clients that will appear in the system from the start to the end of training. Let $\tau(i) \in \{1, \dots, K\}$ denote the types of clients. Based on the types of clients, we can further simplify the expressions $\mathbb{P}(d \in \mathbb{D}^{(g)})$ and $\mathbb{P}(d \in \mathbb{D}^{(g+1)})$ as follows:

$$\mathbb{P}(d \in \mathbb{D}^{(g+1)}) = \mathbb{P}(d \in \cup_k \mathbb{D}_k^{(g+1)}) \leq \sum_{k \in \mathbb{K}^{(g+1)}} \mathbb{P}(d \in \mathbb{D}_k^{(g+1)}) \quad (21)$$

$$= \sum_{k \in \mathbb{K}^{(g+1)}} \mathbb{P}(X_k = d) = \sum_{k \in \mathbb{K}^{(g+1)}} q_{\tau(i)}(d). \quad (22)$$

On the other hand, we have the following as a result of the inclusion-exclusion principle:

$$\mathbb{P}(d \in \mathbb{D}^{(g)}) = \mathbb{P}(d \in \cup_k \mathbb{D}_k^{(g)}) \quad (23)$$

$$\geq \sum_{k \in \mathbb{K}^{(g)}} \mathbb{P}(d \in \mathbb{D}_k^{(g)}) - \sum_{i, j \in \mathbb{K}^{(g)}, i \neq j} \mathbb{P}((d \in \mathbb{D}_i^{(g)}) \cap (d \in \mathbb{D}_j^{(g)})). \quad (24)$$

Since the local data samples are independently distributed, the last term of the previous inequality can be easily expressed:

$$\sum_{i, j \in \mathbb{K}^{(g)}, i \neq j} \mathbb{P}((d \in \mathbb{D}_i^{(g)}) \cap (d \in \mathbb{D}_j^{(g)})) = \sum_{i, j \in \mathbb{K}^{(g)}, i \neq j} \mathbb{P}(d \in \mathbb{D}_i^{(g)}) \mathbb{P}(d \in \mathbb{D}_j^{(g)}) \quad (25)$$

$$= \sum_{i, j \in \mathbb{K}^{(g)}, i \neq j} q_{\tau(i)}(d) q_{\tau(j)}(d). \quad (26)$$

Therefore, we have:

$$\mathbb{P}(d \in \mathbb{D}^{(g)}) \geq \sum_{k \in \mathbb{K}^{(g)}} q_{\tau(i)}(d) - \sum_{i, j \in \mathbb{K}^{(g)}, i \neq j} q_{\tau(i)}(d) q_{\tau(j)}(d) \quad (27)$$

Then, we have the upper bound on B_1 :

$$\frac{D^{(g)} \mathbb{P}(d \in \mathbb{D}^{(g+1)}) - D^{(g+1)} \mathbb{P}(d \in \mathbb{D}^{(g)})}{D^{(g+1)} D^{(g)}} \quad (28)$$

$$\leq \frac{D^{(g)} \sum_{k \in \mathbb{K}^{(g+1)}} q_{\tau(i)}(d) + D^{(g+1)} \left(\sum_{\substack{i,j \in \mathbb{K}^{(g)} \\ i \neq j}} q_{\tau(i)}(d) q_{\tau(j)}(d) - \sum_{k \in \mathbb{K}^{(g)}} q_{\tau(i)}(d) \right)}{D^{(g+1)} D^{(g)}} \quad (29)$$

$$= \psi^{(g+1,g)}(d) \quad (30)$$

Since $\|\mathbb{E}[\nabla F^{(g)}(\mathbf{w})] - \mathbb{E}[\nabla F^{(g+1)}(\mathbf{w})]\| = \|\mathbb{E}[\nabla F^{(g+1)}(\mathbf{w})] - \mathbb{E}[\nabla F^{(g)}(\mathbf{w})]\|$, we have

$$B \leq C \left\| \sum_{d \in \mathbb{D}} \min\{\psi^{(g+1,g)}(d), \psi^{(g,g+1)}(d)\} \right\| \quad (31)$$

$$\leq C \left\| \sum_{d \in \mathbb{D}} \min\{\psi^{(g+1,g)}(d), \psi^{(g,g+1)}(d)\} \right\| \quad (32)$$

Now, we derive expressions for A and C . If we assume that gradient of the loss function is bounded by C on a compact set Ω , and view the Hoeffding's inequality as the complement of the Cumulative Density Function (CDF), we have the following result by using $\mathbb{E}[X] = \int_0^\infty [1 - F_X(x)] dx$

$$\mathbb{E}\|\nabla F^{(g)}(\mathbf{w}) - \mathbb{E}[\nabla F^{(g)}(\mathbf{w})]\| \leq \sqrt{\frac{C\pi}{12D^{(g)}}} \quad (33)$$

Similarly,

$$\mathbb{E}\|\nabla F^{(g+1)}(\mathbf{w}) - \mathbb{E}[\nabla F^{(g+1)}(\mathbf{w})]\| \leq \sqrt{\frac{C\pi}{12D^{(g+1)}}} \quad (34)$$

Put all things together, we have proved

$$\begin{aligned} \mathbb{E}\|\mathbf{w}^{(g)*} - \mathbf{w}^{(g+1)*}\| &\leq \frac{1}{\mu} \left(\sqrt{\frac{C\pi}{12D^{(g)}}} + \sqrt{\frac{C\pi}{12D^{(g+1)}}} \right) \\ &+ \frac{C}{\mu} \left| \sum_{d \in \mathbb{D}} \min\{\psi^{(g,g+1)}(d), \psi^{(g+1,g)}(d)\} \right| \end{aligned} \quad (35)$$

□

B PROOF OF THEOREM 1

We replicate the statement of Theorem 1 again for clarity.

Theorem 1. *If for all clients $k \in \mathbb{K}^{(g)}$, all rounds $g \in \mathbb{G}$, all model parameters $\mathbf{w} \in \mathbb{R}^M$, and all data $d \in \mathbb{D}$, the gradient of the loss function $\nabla \ell$ is bounded on a compact set Ω which contains the possible values of the gradient during model training, i.e. $\|\nabla \ell(\mathbf{w}, d)\| \leq C$, $\forall \mathbf{w} \in \Omega$, then we have the following recursive relationship between two consecutive optimality gap*

$$\begin{aligned} \mathbb{E}\|\mathbf{w}^{(g+1)} - \mathbf{w}^{(g+1)*}\| &\leq 2 \left(1 - \frac{1}{2} \mu \eta^{(g)} \left(\sum_{k \in \mathbb{K}^{(g)}} \frac{D_k^{(g)} e_k^{(g)}}{D^{(g)}} \right) \right) \mathbb{E}\|\mathbf{w}^{(g)} - \mathbf{w}^{(g)*}\| \\ &+ \left(2 + \mu \eta^{(g)} \right) C^2 \left(\sum_{k \in \mathbb{K}^{(g)}} \frac{D_k^{(g)} e_k^{(g)}}{D^{(g)}} \right) \sum_{k \in \mathbb{K}^{(g)}} \frac{D_k^{(g)} (e_k^{(g)} - 1) e_k^{(g)} (2e_k^{(g)} - 1)}{D^{(g)} 3} \\ &+ 2\eta^{(g)} \sum_{k \in \mathbb{K}^{(g)}} \frac{D_k^{(g)} (e_k^{(g)})^2 \sigma_k^2}{D^{(g)}} + 2\eta^{(g)} \left(\sum_{k \in \mathbb{K}^{(g)}} \frac{D_k^{(g)} (L\eta^{(g)} e_k^{(g)} + 2L\eta^{(g)} + 1) e_k^{(g)}}{D^{(g)}} \Gamma_k^{(g)} \right) \\ &+ \frac{2}{\mu} \left(\sqrt{\frac{C\pi}{12D^{(g)}}} + \sqrt{\frac{C\pi}{12D^{(g+1)}}} \right) + \frac{2C}{\mu} \left| \sum_{d \in \mathbb{D}} \min\{\psi^{(g,g+1)}(d), \psi^{(g+1,g)}(d)\} \right| \end{aligned} \quad (36)$$

Proof: By our global aggregation rules and the local model training rule, we have

$$\mathbf{w}^{(g+1)} = \sum_{k \in \mathbb{K}^{(g)}} \frac{D_k^{(g)}}{D^{(g)}} \left(\mathbf{w}^{(g)} - \eta^{(g)} \sum_{h=1}^{e_k^{(g)}} \nabla \tilde{F}_k^{(g)} \left(\mathbf{w}_k^{(g),h-1} \right) \right) \quad (37)$$

$$= \mathbf{w}^{(g)} - \eta^{(g)} \sum_{k \in \mathbb{K}^{(g)}} \frac{D_k^{(g)}}{D^{(g)}} \left(\sum_{h=1}^{e_k^{(g)}} \nabla \tilde{F}_k^{(g)} \left(\mathbf{w}_k^{(g),h-1} \right) \right) \quad (38)$$

$$\triangleq \mathbf{w}^{(g)} - \eta^{(g)} \nabla \tilde{F}^{(g)} \quad (39)$$

where we use $\nabla \tilde{F}_k^{(g)} \left(\mathbf{w}_k^{(g),h-1} \right)$ to denote the stochastic gradient and $\nabla \tilde{F}^{(g)}$ to denote $\sum_{k \in \mathbb{K}^{(g)}} \frac{D_k^{(g)}}{D^{(g)}} \left(\sum_{h=1}^{e_k^{(g)}} \nabla \tilde{F}_k^{(g)} \left(\mathbf{w}_k^{(g),h-1} \right) \right)$ for simplicity.

Next, we relate the optimality gap at round $g+1$ to the optimality at round g :

$$\|\mathbf{w}^{(g+1)} - \mathbf{w}^{(g+1)*}\|^2 \quad (40)$$

$$= \|\mathbf{w}^{(g+1)} - \mathbf{w}^{(g)*} + \mathbf{w}^{(g)*} - \mathbf{w}^{(g+1)*}\|^2 \quad (41)$$

$$\leq 2\|\mathbf{w}^{(g+1)} - \mathbf{w}^{(g)*}\|^2 + 2\|\mathbf{w}^{(g)*} - \mathbf{w}^{(g+1)*}\|^2. \quad (42)$$

Similarly, we use $\nabla F_k^{(g)} \left(\mathbf{w}_k^{(g),h-1} \right)$ to denote the gradient computed using the entire dataset and $\nabla F^{(g)}$ to denote $\sum_{k \in \mathbb{K}^{(g)}} \frac{D_k^{(g)}}{D^{(g)}} \left(\sum_{h=1}^{e_k^{(g)}} \nabla F_k^{(g)} \left(\mathbf{w}_k^{(g),h-1} \right) \right)$ for simplicity. We can expand the first term further:

$$\|\mathbf{w}^{(g+1)} - \mathbf{w}^{(g)*}\|^2 \quad (43)$$

$$= \|\mathbf{w}^{(g)} - \eta^{(g)} \nabla \tilde{F}^{(g)} - \mathbf{w}^{(g)*}\|^2 \quad (44)$$

$$= \|\mathbf{w}^{(g)} - \eta^{(g)} \nabla \tilde{F}^{(g)} - \mathbf{w}^{(g)*} - \eta^{(g)} \nabla F^{(g)} + \eta^{(g)} \nabla F^{(g)}\|^2 \quad (45)$$

$$= \|\mathbf{w}^{(g)} - \eta^{(g)} \nabla \tilde{F}^{(g)} - \mathbf{w}^{(g)*}\|^2 + (\eta^{(g)})^2 \|\nabla \tilde{F}^{(g)} - \nabla F^{(g)}\|^2 \quad (46)$$

$$+ 2\eta^{(g)} \left\langle \mathbf{w}^{(g)} - \mathbf{w}^{(g)*} - \eta^{(g)} \nabla F^{(g)}, \nabla \tilde{F}^{(g)} - \nabla F^{(g)} \right\rangle \quad (47)$$

$$= \|\mathbf{w}^{(g)} - \mathbf{w}^{(g)*}\|^2 - 2\eta^{(g)} \left\langle \mathbf{w}^{(g)} - \mathbf{w}^{(g)*}, \nabla F^{(g)} \right\rangle + (\eta^{(g)})^2 \|\nabla F^{(g)}\|^2 \quad (48)$$

$$+ (\eta^{(g)})^2 \|\nabla \tilde{F}^{(g)} - \nabla F^{(g)}\|^2 + 2\eta^{(g)} \left\langle \mathbf{w}^{(g)} - \mathbf{w}^{(g)*} - \eta^{(g)} \nabla F^{(g)}, \nabla \tilde{F}^{(g)} - \nabla F^{(g)} \right\rangle \quad (49)$$

$$= \|\mathbf{w}^{(g)} - \mathbf{w}^{(g)*}\|^2 - \underbrace{2\eta^{(g)} \left\langle \mathbf{w}^{(g)} - \mathbf{w}^{(g)*}, \nabla F^{(g)} \right\rangle}_{A_1} + \underbrace{(\eta^{(g)})^2 \|\nabla F^{(g)}\|^2}_{A_2} \quad (50)$$

$$+ \underbrace{(\eta^{(g)})^2 \|\nabla \tilde{F}^{(g)} - \nabla F^{(g)}\|^2}_{A_3} + \underbrace{2\eta^{(g)} \left\langle \mathbf{w}^{(g)} - \mathbf{w}^{(g)*} - \eta^{(g)} \nabla F^{(g)}, \nabla \tilde{F}^{(g)} - \nabla F^{(g)} \right\rangle}_{A_4}. \quad (51)$$

Note that $\mathbb{E}[A_4] = 0$ because $\mathbb{E}[\nabla \tilde{F}^{(g)} - \nabla F^{(g)}] = 0$. Now, let's expand A_1 and A_2 :

$$A_2 = (\eta^{(g)})^2 \left\| \sum_{k \in \mathbb{K}^{(g)}} \frac{D_k^{(g)}}{D^{(g)}} \sum_{h=1}^{e_k^{(g)}} \nabla F_k^{(g)} \left(\mathbf{w}_k^{(g),h-1} \right) \right\|^2 \quad (52)$$

$$\leq (\eta^{(g)})^2 \sum_{k \in \mathbb{K}^{(g)}} \frac{D_k^{(g)}}{D^{(g)}} \left\| \sum_{h=1}^{e_k^{(g)}} \nabla F_k^{(g)} \left(\mathbf{w}_k^{(g),h-1} \right) \right\|^2 \quad (53)$$

$$\leq (\eta^{(g)})^2 \sum_{k \in \mathbb{K}^{(g)}} \frac{D_k^{(g)}}{D^{(g)}} e_k^{(g)} \sum_{h=1}^{e_k^{(g)}} \|\nabla F_k^{(g)}(\mathbf{w}_k^{(g),h-1})\|^2 \quad (54)$$

$$\leq 2L(\eta^{(g)})^2 \sum_{k \in \mathbb{K}^{(g)}} \frac{D_k^{(g)}}{D^{(g)}} e_k^{(g)} \sum_{h=1}^{e_k^{(g)}} (\nabla F_k^{(g)}(\mathbf{w}_k^{(g),h-1}) - \nabla F_k^{(g)*}). \quad (55)$$

Now, expanding A_1 :

$$A_1 = -2\eta^{(g)} \langle \mathbf{w}^{(g)} - \mathbf{w}^{(g)*}, \nabla F^{(g)} \rangle \quad (56)$$

$$= -2\eta^{(g)} \sum_{k \in \mathbb{K}^{(g)}} \frac{D_k^{(g)}}{D^{(g)}} \sum_{h=1}^{e_k^{(g)}} \langle \mathbf{w}^{(g)} - \mathbf{w}^{(g)*}, \nabla F_k^{(g)}(\mathbf{w}_k^{(g),h-1}) \rangle \quad (57)$$

$$= -2\eta^{(g)} \underbrace{\sum_{k \in \mathbb{K}^{(g)}} \frac{D_k^{(g)}}{D^{(g)}} \sum_{h=1}^{e_k^{(g)}} \langle \mathbf{w}^{(g)} - \mathbf{w}_k^{(g),h-1}, \nabla F_k^{(g)}(\mathbf{w}_k^{(g),h-1}) \rangle}_{A_{11}} \quad (58)$$

$$-2\eta^{(g)} \underbrace{\sum_{k \in \mathbb{K}^{(g)}} \frac{D_k^{(g)}}{D^{(g)}} \sum_{h=1}^{e_k^{(g)}} \langle \mathbf{w}_k^{(g),h-1} - \mathbf{w}^{(g)*}, \nabla F_k^{(g)}(\mathbf{w}_k^{(g),h-1}) \rangle}_{A_{12}}. \quad (59)$$

We then expand A_{11} and A_{12} :

$$A_{11} = -2\eta^{(g)} \sum_{k \in \mathbb{K}^{(g)}} \frac{D_k^{(g)}}{D^{(g)}} \sum_{h=1}^{e_k^{(g)}} \langle \mathbf{w}_k^{(g)} - \mathbf{w}_k^{(g),h-1}, \nabla F_k^{(g)}(\mathbf{w}_k^{(g),h-1}) \rangle \quad (60)$$

$$\leq \sum_{k \in \mathbb{K}^{(g)}} \frac{D_k^{(g)}}{D^{(g)}} \sum_{h=1}^{e_k^{(g)}} 2\eta^{(g)} \|\mathbf{w}_k^{(g)} - \mathbf{w}_k^{(g),h-1}\| \|\nabla F_k^{(g)}(\mathbf{w}_k^{(g),h-1})\| \quad (61)$$

$$\leq \sum_{k \in \mathbb{K}^{(g)}} \frac{D_k^{(g)}}{D^{(g)}} \sum_{h=1}^{e_k^{(g)}} \eta^{(g)} \left(\frac{1}{\eta^{(g)}} \|\mathbf{w}_k^{(g)} - \mathbf{w}_k^{(g),h-1}\|^2 + \eta^{(g)} \|\nabla F_k^{(g)}(\mathbf{w}_k^{(g),h-1})\|^2 \right) \quad (62)$$

$$\leq \sum_{k \in \mathbb{K}^{(g)}} \frac{D_k^{(g)}}{D^{(g)}} \sum_{h=1}^{e_k^{(g)}} \left(\|\mathbf{w}_k^{(g)} - \mathbf{w}_k^{(g),h-1}\|^2 + (\eta^{(g)})^2 \|\nabla F_k^{(g)}(\mathbf{w}_k^{(g),h-1})\|^2 \right). \quad (63)$$

$$A_{12} = -2\eta^{(g)} \sum_{k \in \mathbb{K}^{(g)}} \frac{D_k^{(g)}}{D^{(g)}} \sum_{h=1}^{e_k^{(g)}} \langle \mathbf{w}_k^{(g),h-1} - \mathbf{w}^{(g)*}, \nabla F_k^{(g)}(\mathbf{w}_k^{(g),h-1}) \rangle \quad (64)$$

$$\leq -2\eta^{(g)} \sum_{k \in \mathbb{K}^{(g)}} \frac{D_k^{(g)}}{D^{(g)}} \sum_{h=1}^{e_k^{(g)}} \left(F_k^{(g)}(\mathbf{w}_k^{(g),h-1}) - F_k^{(g)}(\mathbf{w}_k^{(g)*}) + \frac{\mu}{2} \|\mathbf{w}_k^{(g),h-1} - \mathbf{w}^{(g)*}\|^2 \right). \quad (65)$$

Combining A_{11} and A_{12} , we have:

$$A_1 = \sum_{k \in \mathbb{K}^{(g)}} \frac{D_k^{(g)}}{D^{(g)}} \sum_{h=1}^{e_k^{(g)}} \left(\|\mathbf{w}^{(g)} - \mathbf{w}_k^{(g),h-1}\|^2 + (\eta^{(g)})^2 \|\nabla F_k^{(g)}(\mathbf{w}_k^{(g),h-1})\|^2 \right) \quad (66)$$

$$-2\eta^{(g)} \left(F_k^{(g)}(\mathbf{w}_k^{(g),h-1}) - F_k^{(g)}(\mathbf{w}^{(g)*}) - \eta^{(g)} \mu \|\mathbf{w}_k^{(g),h-1} - \mathbf{w}^{(g)*}\|^2 \right). \quad (67)$$

Next, we combine A_1 and A_2 :

$$A_1 + A_2 = 2L(\eta^{(g)})^2 \underbrace{\sum_{k \in \mathbb{K}^{(g)}} \frac{D_k^{(g)}}{D^{(g)}} (e_k^{(g)} + 1) \sum_{h=1}^{e_k^{(g)}} \left(F_k^{(g)}(\mathbf{w}_k^{(g)}) - F_k^{(g)*} \right)}_{B_1 \text{ (first term)}} \quad (68)$$

$$\underbrace{-2\eta^{(g)} \sum_{k \in \mathbb{K}^{(g)}} \frac{D_k^{(g)}}{D^{(g)}} \left(\sum_{h=1}^{e_k^{(g)}} \left(F_k^{(g)}(\mathbf{w}_k^{(g),h-1}) - F_k^{(g)}(\mathbf{w}^{(g)*}) \right) \right)}_{B_1 \text{ (second term)}} \quad (69)$$

$$+ \sum_{k \in \mathbb{K}^{(g)}} \frac{D_k^{(g)}}{D^{(g)}} \sum_{h=1}^{e_k^{(g)}} \|\mathbf{w}^{(g)} - \mathbf{w}_k^{(g),h-1}\|^2 \quad (70)$$

$$\underbrace{-\eta^{(g)} \mu \sum_{k \in \mathbb{K}^{(g)}} \frac{D_k^{(g)}}{D^{(g)}} \sum_{h=1}^{e_k^{(g)}} \|\mathbf{w}_k^{(g),h-1} - \mathbf{w}^{(g)*}\|^2}_{B_2}. \quad (71)$$

For the third item, we further simplify:

$$\|\mathbf{w}_k^{(g),h-1} - \mathbf{w}^{(g)*}\|^2 = \|\mathbf{w}_k^{(g),h-1} - \mathbf{w}^{(g)} + \mathbf{w}^{(g)} - \mathbf{w}^{(g)*}\|^2 \quad (72)$$

$$= \|\mathbf{w}_k^{(g),h-1} - \mathbf{w}^{(g)}\|^2 + \|\mathbf{w}^{(g)} - \mathbf{w}^{(g)*}\|^2 \quad (73)$$

$$+ 2\langle \mathbf{w}_k^{(g),h-1} - \mathbf{w}^{(g)}, \mathbf{w}^{(g)} - \mathbf{w}^{(g)*} \rangle \quad (74)$$

$$\geq \|\mathbf{w}_k^{(g),h-1} - \mathbf{w}^{(g)}\|^2 + \|\mathbf{w}^{(g)} - \mathbf{w}^{(g)*}\|^2 \quad (75)$$

$$- 2\|\mathbf{w}_k^{(g),h-1} - \mathbf{w}^{(g)}\| \cdot \|\mathbf{w}^{(g)} - \mathbf{w}^{(g)*}\| \quad (76)$$

$$\geq \|\mathbf{w}_k^{(g),h-1} - \mathbf{w}^{(g)}\|^2 + \|\mathbf{w}^{(g)} - \mathbf{w}^{(g)*}\|^2 \quad (77)$$

$$- 2\|\mathbf{w}_k^{(g),h-1} - \mathbf{w}^{(g)}\| - \frac{1}{2}\|\mathbf{w}^{(g)} - \mathbf{w}^{(g)*}\|^2 \quad (78)$$

$$\geq -\|\mathbf{w}_k^{(g),h-1} - \mathbf{w}^{(g)}\| + \frac{1}{2}\|\mathbf{w}^{(g)} - \mathbf{w}^{(g)*}\|^2. \quad (79)$$

From this, we derive an upper bound on B_2 :

$$B_2 \leq -\frac{\eta^{(g)} \mu}{2} \left(\sum_{k \in \mathbb{K}^{(g)}} \frac{D_k^{(g)} e_k^{(g)}}{D^{(g)}} \right) \|\mathbf{w}^{(g)} - \mathbf{w}^{(g)*}\|^2 \quad (80)$$

$$+ \mu \eta^{(g)} \sum_{k \in \mathbb{K}^{(g)}} \frac{D_k^{(g)}}{D^{(g)}} \sum_{h=1}^{e_k^{(g)}} \|\mathbf{w}_k^{(g),h-1} - \mathbf{w}^{(g)}\|^2. \quad (81)$$

Plug the expressions for the third item and B_2 back into $A_1 + A_2$:

$$A_1 + A_2 \leq B_1 + (1 + \mu \eta^{(g)}) \sum_{k \in \mathbb{K}^{(g)}} \frac{D_k^{(g)}}{D^{(g)}} \sum_{h=1}^{e_k^{(g)}} \|\mathbf{w}_k^{(g),h-1} - \mathbf{w}^{(g)}\|^2 \quad (82)$$

$$- \frac{\eta^{(g)}\mu}{2} \left(\sum_{k \in \mathbb{K}^{(g)}} \frac{D_k^{(g)} e_k^{(g)}}{D^{(g)}} \right) \|\mathbf{w}^{(g)} - \mathbf{w}^{(g)*}\|^2. \quad (83)$$

We then expand B_1 as follows:

$$B_1 = 2L(\eta^{(g)})^2 \sum_{k \in \mathbb{K}^{(g)}} \frac{D_k^{(g)}}{D^{(g)}} (e_k^{(g)} + 1) \sum_{h=1}^{e_k^{(g)}} \left(F_k^{(g)}(\mathbf{w}_k^{(g)}) - F_k^{(g)*} \right) \quad (84)$$

$$+ \underbrace{\sum_{k \in \mathbb{K}^{(g)}} \frac{D_k^{(g)}}{D^{(g)}} \sum_{h=1}^{e_k^{(g)}} \left(2L(\eta^{(g)})^2 (e_k^{(g)} + 1) - 2\eta^{(g)} \right) \left(F_k^{(g)}(\mathbf{w}_k^{(g),h-1}) - F_k^{(g)}(\mathbf{w}^{(g)*}) \right)}_{-V_k^{(g)}}}_{B_{11}}. \quad (85)$$

We expand B_{11} further:

$$B_{11} = -V_k^{(g)} \left(F_k^{(g)}(\mathbf{w}_k^{(g),h-1}) - F_k^{(g)}(\mathbf{w}^{(g)*}) \right) \quad (86)$$

$$= -V_k^{(g)} \left(F_k^{(g)}(\mathbf{w}_k^{(g),h-1}) - F_k^{(g)}(\mathbf{w}^{(g)}) + F_k^{(g)}(\mathbf{w}^{(g)}) - F_k^{(g)}(\mathbf{w}^{(g)*}) \right) \quad (87)$$

$$\leq -V_k^{(g)} \left(\left\langle \nabla F_k^{(g)}(\mathbf{w}^{(g)}), \mathbf{w}_k^{(g),h-1} - \mathbf{w}^{(g)} \right\rangle + \frac{\mu}{2} \|\mathbf{w}_k^{(g),h-1} - \mathbf{w}^{(g)}\|^2 \right) \quad (88)$$

$$- V_k^{(g)} \left(F_k^{(g)}(\mathbf{w}^{(g)}) - F_k^{(g)}(\mathbf{w}^{(g)*}) \right) \quad (89)$$

$$\leq V_k^{(g)} \left\langle \mathbf{w}_k^{(g)} - \mathbf{w}_k^{(g),h-1}, \nabla F_k^{(g)}(\mathbf{w}^{(g)}) \right\rangle - \frac{\mu V_k^{(g)}}{2} \|\mathbf{w}_k^{(g),h-1} - \mathbf{w}^{(g)}\|^2 \quad (90)$$

$$- V_k^{(g)} \left(F_k^{(g)}(\mathbf{w}^{(g)}) - F_k^{(g)}(\mathbf{w}^{(g)*}) \right) \quad (91)$$

$$\leq \frac{V_k^{(g)}\eta^{(g)}}{2} \|\nabla F_k^{(g)}(\mathbf{w}^{(g)})\|^2 + \frac{V_k^{(g)}}{2\eta^{(g)}} \|\mathbf{w}_k^{(g)} - \mathbf{w}_k^{(g),h-1}\|^2 \quad (92)$$

$$- \frac{\mu V_k^{(g)}}{2} \|\mathbf{w}_k^{(g),h-1} - \mathbf{w}^{(g)}\|^2 - V_k^{(g)} \left(F_k^{(g)}(\mathbf{w}^{(g)}) - F_k^{(g)}(\mathbf{w}^{(g)*}) \right) \quad (93)$$

$$\leq V_k^{(g)} L\eta^{(g)} \left(F_k^{(g)}(\mathbf{w}^{(g)}) - F_k^{(g)*} \right) + \frac{V_k^{(g)}(1 - \mu\eta^{(g)})}{2\eta^{(g)}} \|\mathbf{w}^{(g)} - \mathbf{w}_k^{(g),h-1}\|^2 \quad (94)$$

$$- V_k^{(g)} \left(F_k^{(g)}(\mathbf{w}^{(g)}) - F_k^{(g)}(\mathbf{w}^{(g)*}) \right) \quad (95)$$

$$\leq V_k^{(g)} L\eta^{(g)} \left(F_k^{(g)}(\mathbf{w}^{(g)*}) - F_k^{(g)*} \right) + \|\mathbf{w}^{(g)} - \mathbf{w}_k^{(g),h-1}\|^2 \quad (96)$$

$$+ V_k^{(g)}(1 - L\eta^{(g)}) \left(F_k^{(g)}(\mathbf{w}^{(g)*}) - F_k^{(g)}(\mathbf{w}^{(g)}) \right) \quad (97)$$

$$\leq V_k^{(g)} L\eta^{(g)} \left(F_k^{(g)}(\mathbf{w}^{(g)*}) - F_k^{(g)*} \right) + \|\mathbf{w}^{(g)} - \mathbf{w}_k^{(g),h-1}\|^2 \quad (98)$$

$$+ V_k^{(g)}(1 - L\eta^{(g)}) \left(F_k^{(g)}(\mathbf{w}^{(g)*}) - F_k^{(g)*} + \underbrace{F_k^{(g)*} - F_k^{(g)}(\mathbf{w}^{(g)})}_{\leq 0} \right) \quad (99)$$

$$\leq V_k^{(g)} L\eta^{(g)} \left(F_k^{(g)}(\mathbf{w}^{(g)*}) - F_k^{(g)*} \right) + \|\mathbf{w}^{(g)} - \mathbf{w}_k^{(g),h-1}\|^2 \quad (100)$$

$$+ V_k^{(g)} \left(F_k^{(g)}(\mathbf{w}^{(g)*}) - F_k^{(g)*} \right) \quad (101)$$

$$\leq V_k^{(g)} \left(L\eta^{(g)} + 1 \right) \left(F_k^{(g)}(\mathbf{w}^{(g)*}) - F_k^{(g)*} \right) + \|\mathbf{w}^{(g)} - \mathbf{w}_k^{(g),h-1}\|^2. \quad (102)$$

Substituting the expression for B_{11} back into B_1 and noting that $V_k^{(g)} \leq 2\eta^{(g)}$, we have:

$$B_1 = 2L(\eta^{(g)})^2 \sum_{k \in \mathbb{K}^{(g)}} \frac{D_k^{(g)}}{D^{(g)}} (e_k^{(g)} + 1) \sum_{h=1}^{e_k^{(g)}} \left(F_k^{(g)}(\mathbf{w}^{(g)*}) - F_k^{(g)*} \right) \quad (103)$$

$$+ \sum_{k \in \mathbb{K}^{(g)}} \frac{D_k^{(g)}}{D^{(g)}} \sum_{h=1}^{e_k^{(g)}} 2\eta^{(g)} \left(L\eta^{(g)} + 1 \right) \left(F_k^{(g)}(\mathbf{w}^{(g)*}) - F_k^{(g)*} \right) \quad (104)$$

$$+ \sum_{k \in \mathbb{K}^{(g)}} \frac{D_k^{(g)}}{D^{(g)}} \sum_{h=1}^{e_k^{(g)}} \|\mathbf{w}^{(g)} - \mathbf{w}_k^{(g),h-1}\|^2 \quad (105)$$

$$= 2\eta^{(g)} \sum_{k \in \mathbb{K}^{(g)}} \frac{D_k^{(g)} \left(L\eta^{(g)} e_k^{(g)} + 2L\eta^{(g)} + 1 \right)}{D^{(g)}} \sum_{h=1}^{e_k^{(g)}} \left(F_k^{(g)}(\mathbf{w}^{(g)*}) - F_k^{(g)*} \right) \quad (106)$$

$$+ \sum_{k \in \mathbb{K}^{(g)}} \frac{D_k^{(g)}}{D^{(g)}} \sum_{h=1}^{e_k^{(g)}} \|\mathbf{w}^{(g)} - \mathbf{w}_k^{(g),h-1}\|^2 \quad (107)$$

$$= 2\eta^{(g)} \sum_{k \in \mathbb{K}^{(g)}} \frac{D_k^{(g)} \left(L\eta^{(g)} e_k^{(g)} + 2L\eta^{(g)} + 1 \right)}{D^{(g)}} e_k^{(g)} \Gamma_k^{(g)} \quad (108)$$

$$+ \sum_{k \in \mathbb{K}^{(g)}} \frac{D_k^{(g)}}{D^{(g)}} \sum_{h=1}^{e_k^{(g)}} \|\mathbf{w}^{(g)} - \mathbf{w}_k^{(g),h-1}\|^2. \quad (109)$$

Substituting the expression back into $A_1 + A_2$:

$$A_1 + A_2 \leq 2\eta^{(g)} \sum_{k \in \mathbb{K}^{(g)}} \frac{D_k^{(g)} \left(L\eta^{(g)} e_k^{(g)} + 2L\eta^{(g)} + 1 \right)}{D^{(g)}} e_k^{(g)} \Gamma_k^{(g)} \quad (110)$$

$$+ (2 + \mu\eta^{(g)}) \sum_{k \in \mathbb{K}^{(g)}} \frac{D_k^{(g)}}{D^{(g)}} \sum_{h=1}^{e_k^{(g)}} \|\mathbf{w}^{(g)} - \mathbf{w}_k^{(g),h-1}\|^2 \quad (111)$$

$$- \frac{\eta^{(g)} \mu}{2} \left(\sum_{k \in \mathbb{K}^{(g)}} \frac{D_k^{(g)} e_k^{(g)}}{D^{(g)}} \right) \|\mathbf{w}^{(g)} - \mathbf{w}^{(g)*}\|^2. \quad (112)$$

Next, we bound the term $\sum_{h=1}^{e_k^{(g)}} \|\mathbf{w}^{(g)} - \mathbf{w}_k^{(g),h-1}\|^2$:

$$\sum_{h=1}^{e_k^{(g)}} \|\mathbf{w}^{(g)} - \mathbf{w}_k^{(g),h-1}\|^2 = \sum_{h=2}^{e_k^{(g)}} \left\| \sum_{m=0}^{h-2} \nabla F_k^{(g)}(\mathbf{w}_k^{(g),m}) \right\|^2 \quad (113)$$

$$= \sum_{q=0}^{e_k^{(g)}-2} \left\| \sum_{m=0}^q \nabla F_k^{(g)}(\mathbf{w}_k^{(g),m}) \right\|^2 \leq \sum_{q=0}^{e_k^{(g)}-2} (q+1) \sum_{m=0}^q \|\nabla F_k^{(g)}(\mathbf{w}_k^{(g),m})\|^2 \quad (114)$$

$$= \sum_{q=0}^{e_k^{(g)}-2} (q+1)^2 C^2 = C^2 \sum_{q=0}^{e_k^{(g)}-2} (q+1)^2 = \frac{C^2 (e_k^{(g)} - 1) e_k^{(g)} (2e_k^{(g)} - 1)}{6}. \quad (115)$$

Substituting into $A_1 + A_2$, we get:

$$A_1 + A_2 \leq 2\eta^{(g)} \sum_{k \in \mathbb{K}^{(g)}} \frac{D_k^{(g)} (L\eta^{(g)} e_k^{(g)} + 2L\eta^{(g)} + 1)}{D^{(g)}} e_k^{(g)} \Gamma_k^{(g)} \quad (116)$$

$$+ (2 + \mu\eta^{(g)}) \sum_{k \in \mathbb{K}^{(g)}} \frac{D_k^{(g)}}{D^{(g)}} \frac{C^2 (e_k^{(g)} - 1) e_k^{(g)} (2e_k^{(g)} - 1)}{6} \quad (117)$$

$$- \frac{\mu\eta^{(g)}}{2} \left(\sum_{k \in \mathbb{K}^{(g)}} \frac{D_k^{(g)} e_k^{(g)}}{D^{(g)}} \right) \|\mathbf{w}^{(g)} - \mathbf{w}^{(g)*}\|^2. \quad (118)$$

Finally, let's derive the expression for A_3 :

$$A_3 = (\eta^{(g)})^2 \left\| \sum_{k \in \mathbb{K}^{(g)}} \frac{D_k^{(g)}}{D^{(g)}} \sum_{h=1}^{e_k^{(g)}} (\nabla \tilde{F}_k^{(g)} - \nabla F_k^{(g)}) \right\|^2 \quad (119)$$

$$\leq (\eta^{(g)})^2 \sum_{k \in \mathbb{K}^{(g)}} \frac{D_k^{(g)}}{D^{(g)}} \left\| \sum_{h=1}^{e_k^{(g)}} (\nabla \tilde{F}_k^{(g)} - \nabla F_k^{(g)}) \right\|^2 \quad (120)$$

$$\leq \eta^{(g)} \sum_{k \in \mathbb{K}^{(g)}} \frac{D_k^{(g)}}{D^{(g)}} e_k^{(g)} \sum_{h=1}^{e_k^{(g)}} \|\nabla \tilde{F}_k^{(g)} - \nabla F_k^{(g)}\|^2 \quad (121)$$

$$\leq \eta^{(g)} \sum_{k \in \mathbb{K}^{(g)}} \frac{D_k^{(g)}}{D^{(g)}} (e_k^{(g)})^2 \sigma_k^2. \quad (122)$$

Taking the expectation and combining the expressions for A_1 , A_2 , and A_3 , we have:

$$\mathbb{E} \|\mathbf{w}^{(g+1)} - \mathbf{w}^{(g+1)*}\| \leq 2 \left(1 - \frac{1}{2} \mu\eta^{(g)} \left(\sum_{k \in \mathbb{K}^{(g)}} \frac{D_k^{(g)} e_k^{(g)}}{D^{(g)}} \right) \right) \mathbb{E} \|\mathbf{w}^{(g)} - \mathbf{w}^{(g)*}\| \quad (123)$$

$$+ \left(2 + \mu\eta^{(g)} \right) C^2 \left(\sum_{k \in \mathbb{K}^{(g)}} \frac{D_k^{(g)} e_k^{(g)}}{D^{(g)}} \right) \sum_{k \in \mathbb{K}^{(g)}} \frac{D_k^{(g)} (e_k^{(g)} - 1) e_k^{(g)} (2e_k^{(g)} - 1)}{3} \quad (124)$$

$$+ 2\eta^{(g)} \sum_{k \in \mathbb{K}^{(g)}} \frac{D_k^{(g)} (e_k^{(g)})^2 \sigma_k^2}{D^{(g)}} + 2\eta^{(g)} \left(\sum_{k \in \mathbb{K}^{(g)}} \frac{D_k^{(g)} (L\eta^{(g)} e_k^{(g)} + 2L\eta^{(g)} + 1) e_k^{(g)} \Gamma_k^{(g)}}{D^{(g)}} \right) \quad (125)$$

$$+ 2\mathbb{E} \|\mathbf{w}^{(g)*} - \mathbf{w}^{(g+1)*}\|. \quad (126)$$

Plugging the expression in Lemma 1 for the last terms yields

$$\mathbb{E} \|\mathbf{w}^{(g+1)} - \mathbf{w}^{(g+1)*}\| \leq 2 \left(1 - \frac{1}{2} \mu\eta^{(g)} \left(\sum_{k \in \mathbb{K}^{(g)}} \frac{D_k^{(g)} e_k^{(g)}}{D^{(g)}} \right) \right) \mathbb{E} \|\mathbf{w}^{(g)} - \mathbf{w}^{(g)*}\| \quad (127)$$

$$+ \left(2 + \mu\eta^{(g)} \right) C^2 \left(\sum_{k \in \mathbb{K}^{(g)}} \frac{D_k^{(g)} e_k^{(g)}}{D^{(g)}} \right) \sum_{k \in \mathbb{K}^{(g)}} \frac{D_k^{(g)} (e_k^{(g)} - 1) e_k^{(g)} (2e_k^{(g)} - 1)}{3} \quad (128)$$

$$+ 2\eta^{(g)} \sum_{k \in \mathbb{K}^{(g)}} \frac{D_k^{(g)} (e_k^{(g)})^2 \sigma_k^2}{D^{(g)}} + 2\eta^{(g)} \left(\sum_{k \in \mathbb{K}^{(g)}} \frac{D_k^{(g)} (L\eta^{(g)} e_k^{(g)} + 2L\eta^{(g)} + 1) e_k^{(g)}}{D^{(g)}} \Gamma_k^{(g)} \right) \quad (129)$$

$$+ \frac{2}{\mu} \left(\sqrt{\frac{C\pi}{12D^{(g)}}} + \sqrt{\frac{C\pi}{12D^{(g+1)}}} \right) + \frac{2C}{\mu} \left| \sum_{d \in \mathbb{D}} \min\{\psi^{(g,g+1)}(d), \psi^{(g+1,g)}(d)\} \right| \quad (130)$$

□

C MORE EXPERIMENT RESULTS AND DETAILS

Figure 3 presents more results for FedProx with various label distributions, datasets and models.

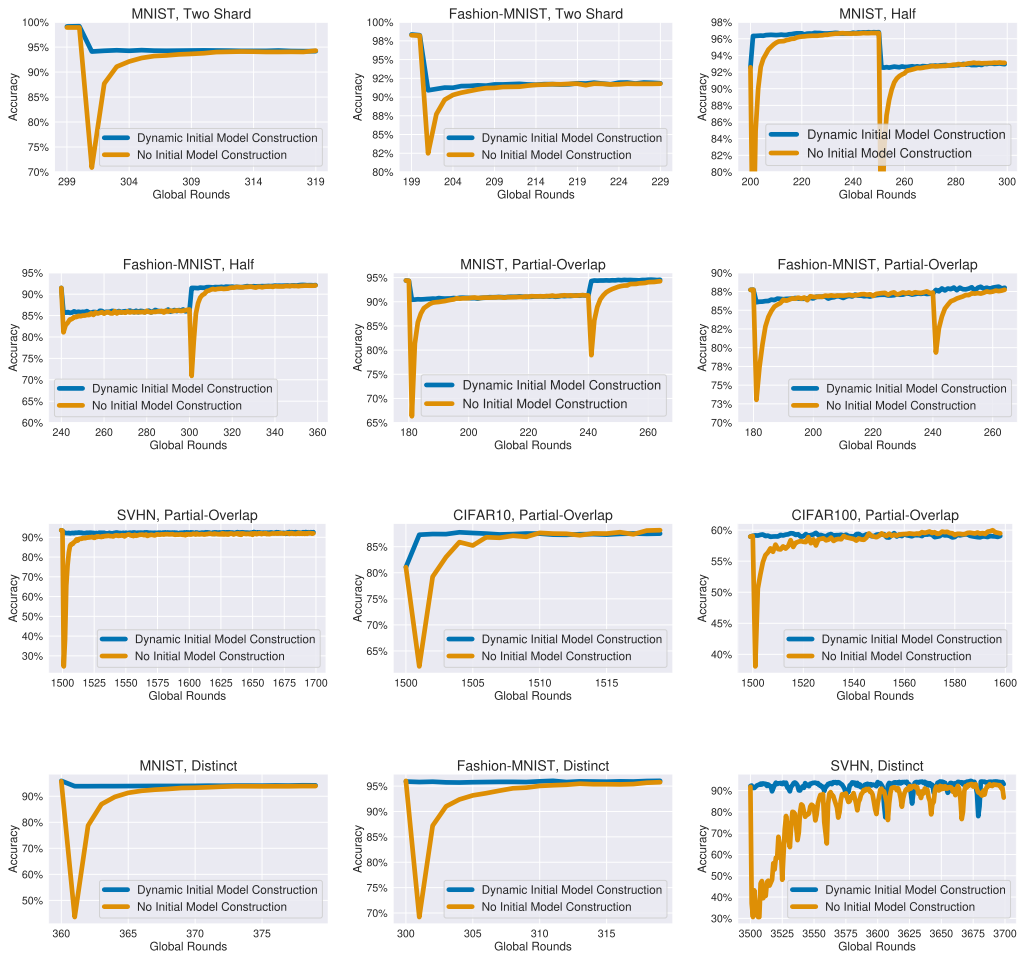


Figure 3: Performance comparison of proposed algorithm for FedProx to the baseline across the remaining examined label distributions, datasets, and models.

Figure 4 presents more results for FedAvg with various label distributions, datasets and models.

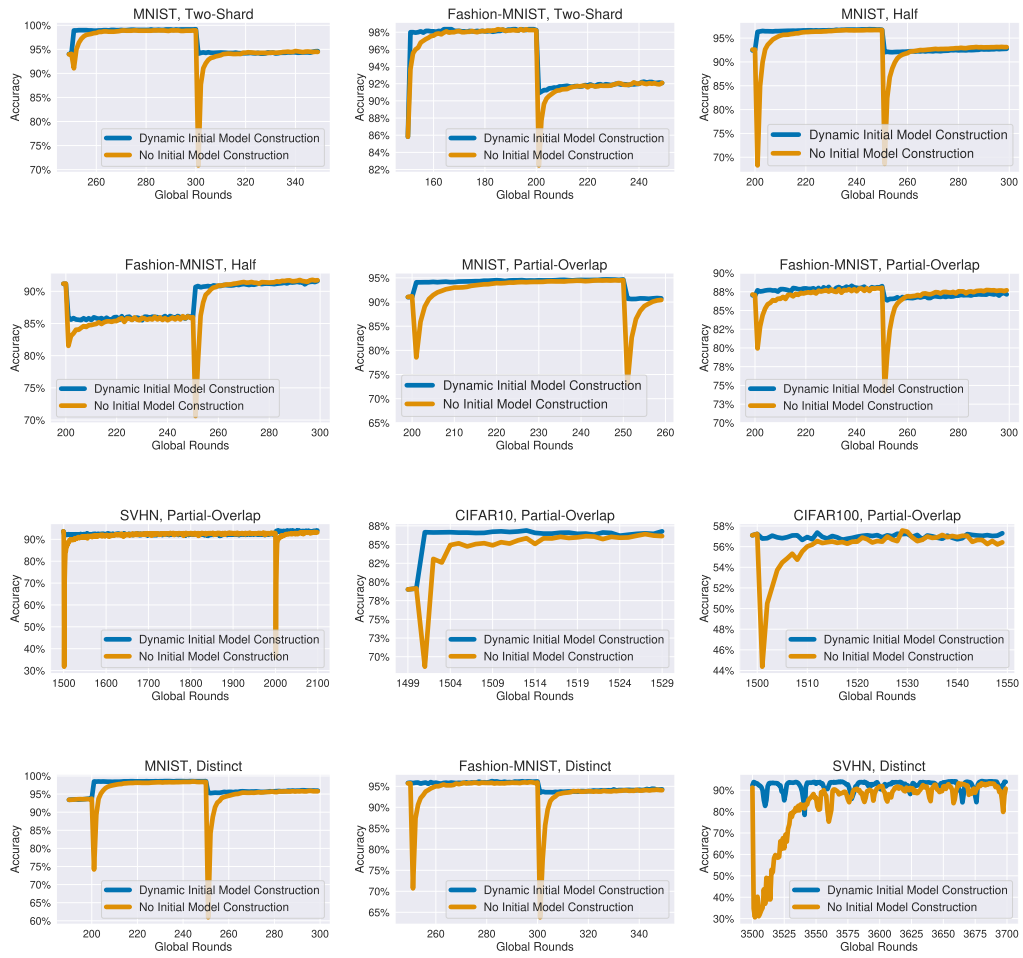


Figure 4: Performance comparison of proposed algorithm for FedProx to the baseline across the remaining examined label distributions, datasets, and models.

C.1 CLIENT PATTERN

For client pattern used in all label distributions, please see Table 2 and 3. Client pattern is the same for FedAvg and FedProx.

Session	Two Shard					Distinct		
	MNIST	Fashion-MNIST	SVHN	CIFAR10	CIFAR100	MNIST	Fashion-MNIST	SVHN
1	[0, 4, 6, 7]	[0, 1, 4, 9]	[1, 5, 6]	[1, 5, 6]	[1, 5, 6]	[0, 1, 2]	[0, 1, 2]	[0, 1, 2]
2	[5]	[5]	[0, 4, 8]	[0, 4, 8]	[0, 2, 3, 9]	[0, 1, 2]	[0, 1, 2]	[0, 1, 2]
3	[0, 4, 6]	[0, 4, 6, 8]	[3]	[1, 2, 3, 5, 6, 9]	[8]	[3, 4, 5]	[3, 4, 5]	[3, 4, 5]
4	[5]	[5]	[1, 4]	[4]	[0, 2, 3, 4, 6, 9]	[6, 7, 8, 9]	[6, 7, 8, 9]	[6, 7, 8, 9]
5	[4, 6, 7]	[0, 4, 6, 7]	[3, 5, 8]	[1, 2, 3, 5, 6, 8]	[5, 8]	[0, 1, 2]	[0, 1, 2]	[0, 1, 2]
6	[5]	[5]	[1, 4, 7]	[4]	[0, 2, 3, 6, 7]	[3, 4, 5]	[3, 4, 5]	[3, 4, 5]
7	[4, 6]	[4, 6]	[5]	[1, 5, 6, 9]	[1, 5, 8]	[6, 7, 8, 9]	[6, 7, 8, 9]	[6, 7, 8, 9]
8	[5]	[5]	[1, 4]	[0, 4]	[0, 2, 7]	[3, 4, 5]	[3, 4, 5]	[3, 4, 5]

Table 2: Client Pattern for Label Distribution Two-Shard and Distinct

Session	Half & Partial-Overlap				
	MNIST	Fashion-MNIST	SVHN	CIFAR10	CIFAR100
1	[0, 1, 2, 3, 4]	[0, 1, 2, 3, 4]	[0, 1, 2, 3, 4]	[0, 1, 2, 3, 4]	[0, 1, 2, 3, 4]
2	[5, 6, 7, 8, 9]	[5, 6, 7, 8, 9]	[5, 6, 7, 8, 9]	[5, 6, 7, 8, 9]	[5, 6, 7, 8, 9]
3	[0, 1, 2, 3, 4]	[0, 1, 2, 3, 4]	[0, 1, 2, 3, 4]	[0, 1, 2, 3, 4]	[0, 1, 2, 3, 4]
4	[5, 6, 7, 8, 9]	[5, 6, 7, 8, 9]	[5, 6, 7, 8, 9]	[5, 6, 7, 8, 9]	[5, 6, 7, 8, 9]
5	[0, 1, 2, 3, 4]	[0, 1, 2, 3, 4]	[0, 1, 2, 3, 4]	[0, 1, 2, 3, 4]	[0, 1, 2, 3, 4]
6	[5, 6, 7, 8, 9]	[5, 6, 7, 8, 9]	[5, 6, 7, 8, 9]	[5, 6, 7, 8, 9]	[5, 6, 7, 8, 9]
7	[0, 1, 2, 3, 4]	[0, 1, 2, 3, 4]	[0, 1, 2, 3, 4]	[0, 1, 2, 3, 4]	[0, 1, 2, 3, 4]
8	[5, 6, 7, 8, 9]	[5, 6, 7, 8, 9]	[5, 6, 7, 8, 9]	[5, 6, 7, 8, 9]	[5, 6, 7, 8, 9]

Table 3: Client Pattern for Label Distribution Half and Partial-Overlap

C.2 MODELS FOR MNIST, FASHION-MNIST, AND SVHN

The model code for MNIST, Fashion-MNIST, and SVHN is as follows.

```

1 class net(nn.Module):
2     def __kinit__(self, dataset_name) -> None:
3         super().__kinit__()
4         if dataset_name == "mnist":
5             self.in_channel = 28 * 28
6         elif dataset_name == "fmnist":
7             self.in_channel = 28 * 28
8         self.out_channel = 10
9         self.net = nn.Linear(self.in_channel, self.out_channel)
10
11     def forward(self, x):
12         x = x.view(-1, x.shape[1] * x.shape[2] * x.shape[3])
13         x = self.net(x)
14         return nn.functional.log_softmax(x, dim=1)

```

Listing 1: Model for MNIST and Fashion-MNIST

```

1 class CNN_SVHN(nn.Module):
2     def __kinit__(self, num_classes=10):
3         super().__kinit__()
4         self.conv1 = nn.Conv2d(in_channels=3, out_channels=32,
5                                 kernel_size=3, padding=1)
6         self.conv2 = nn.Conv2d(in_channels=32, out_channels=64,
7                                 kernel_size=3, padding=1)
8         self.conv3 = nn.Conv2d(in_channels=64, out_channels=128,
9                                 kernel_size=3, padding=1)
9         self.fc1 = nn.Linear(128 * 4 * 4, 256)
10        self.fc2 = nn.Linear(256, num_classes)

```

```
9     self.dropout = nn.Dropout(0.5) # Dropout with a probability
      of 0.5
10
11     def forward(self, x):
12         x = F.relu(F.max_pool2d(self.conv1(x), 2))
13         x = F.relu(F.max_pool2d(self.conv2(x), 2))
14         x = F.relu(F.max_pool2d(self.conv3(x), 2))
15         x = x.view(x.size(0), -1)
16         x = F.relu(self.fc1(x))
17         x = self.dropout(x) # Apply Dropout after the first fully
      connected layer
18         x = self.fc2(x)
19     return x
```

Listing 2: Model for SVHN